NPL Report MATC(A)62

October 2001

Critical Evaluation of Abrasion and Wear Testing of Coatings by Ball Cratering

M G Gee[1], A Gant[1], I Hutchings[2], R Bethke[3],
K Schiffman[3], K Van Acker[4], S Poulat[5],
Y Gachon[6], and J von Stebut[7]

[1]The Materials Centre, National Physical Laboratory
Teddington, Middlesex TW11 0LW, UK

[2]University of Cambridge, Institute for Manufacturing, Dept of Engineering
Mill Street, Cambridge, CB2 1RX, UK

[3]Fraunhofer Institut für Schicht- und Oberflächentechnik
Bienroder Weg 54 E, D-38108 Braunschweig, Germany

[4]VITO, Boertang 200, B-2400
Mol, Belgium

[5]Teer Coatings Ltd, 290 Hartlebury Trading Estate, Hartlebury
Kidderminster, UK

[6]HEF R & D
ZI Sud, Rue Benoit Fourneyron,
Andrezieux Boutheon Cedex, France

[7] Laboratoire de Science et Genie des Surfaces (LSGS)
Ecole des Mines, Nancy F54042, France

SUMMARY

This critical review has been carried out as part of the EU part funded project contract no GRD2000-25020. It examines how abrasion testing for coated materials can be carried out. In particular, it focuses on the ball cratering (or micro-abrasion) test.

The basic principles of the test are explained in respects of the different types of tests that can be carried out. These are

- tests without perforation of coating giving a wear rate for the coating alone.
- tests with perforation where wear rates for coating and substrate can be found independently
- unlubricated sliding wear tests with friction measurement

The effect of different test parameters on the results that are obtained, and the measurements that can be used are discussed.

ISSN 1473 2734

National Physical Laboratory
Teddington, Middlesex, UK, TW11 0LW

Approved on behalf of Managing Director, NPL, by Dr C Lea,
Head of Materials Centre

CONTENTS

1 INTRODUCTION

One of the primary functions for engineering coatings such as TiN and diamond-like-carbon (DLC) is to improve the wear resistance and thus durability of components and products.

To determine these aspects of the performance of coatings, robust wear testing techniques are required.

Traditional techniques such as pin-on-disc or reciprocating sliding wear tests or the dry sand rubber wheel test have been used successfully [1,2], but, particularly for thin hard coatings, there can be considerable difficulties in performing tests [3]. This is often related to the fact that coating thickness constrains the volume or depth of material that can be removed before the coating is perforated. Thus for successful measurements of the wear of the coating, only small amounts of wear can be tolerated. Traditional methods of measurement such as mass loss become ineffective, and even techniques such as profilometry often cannot be used for components with normal engineering finishes as the depth of the wear damage is within the uncertainty of measurement caused by the original roughness of the surface.

One technique that has been considered for assessing the resistance of coatings to single or repeated abrasion events is scratch testing with single or multiple repeat scratches [4,5]. This shows considerable promise as a model test, but will not be considered further here.

This report reviews ball cratering (otherwise known as micro-abrasion testing) which is a promising new technique for assessing the wear resistance of coated and surface engineered components. It was developed from two earlier techniques. These are dimpling to prepare transmission electron microscope samples ready for ion-beam thinning and cap-grinding for the measurement of coating thickness. In both cases spherical depressions were produced.

In ball cratering these techniques have been modified so that wear properties can be determined by performing tests where the test parameters are carefully controlled so that repeatable and reproducible measurements of the wear resistance of materials can be made.

Currently there are no agreed test procedures in place for the use of this test. This is unfortunate as there are now a considerable number of systems installed both in Europe and worldwide (probably in the range 50-150). This lack of control is leading to a lack in reproducibility in results.

To rectify this situation, there are currently major efforts occurring in the USA through ASTM, and Europe through CEN to develop agreed procedures and standards for this test. In CEN a draft standard is now being prepared for publication.

The CRATER collaborative project, which is funded by the EU, has the purpose of validating this draft standard and this review forms the first deliverable from that project.

2 OVERVIEW OF TEST SYSTEMS

Three variants of the test system have emerged. In all the different types of system wear is produced by pressing a rotating wheel or ball against the test sample, and introducing an abrasive suspension into the wear interface (Figure 1). The three variants are described below.

2.1 ROTATING WHEEL (DIMPLER) INSTRUMENTS

Here a spherical depression is produced by rotating the sample under the rotating wheel. To carry out tests effectively it is essential to accurately align the axis of sample rotation with the contact point between the test wheel and the sample. Although this has been achieved [6], the need for exact alignment makes this type of test difficult to carry out.

Tests can also be carried out without rotation of the sample. This ideally leads to a wear scar that has a cylindrical form, but alignment of the sample against the wheel is sometimes difficult to achieve (Figure 2) [7]. Thus wedge shaped scars are produced which become less symmetrical as the mis-alignment increases. If the wheel is shaped with a rounded edge or becomes worn, elliptical or even circular craters are created (Figure 2c).

2.2 THE CAP GRINDING OR FREE BALL SYSTEM

This test system (Figure 3a) uses a free ball which is driven by friction at the contact with a notched drive shaft. Because the ball is not directly driven, there is some uncertainty in the speed of the ball. However, the grip of the ball on the shaft can be improved by the use of rubber driving elements on the shaft [8]. The normal load is generated from the weight of the ball resting on the test sample. It is varied by altering the angle of the sample holding plate. However, it has been found that as the angle is reduced to increase the normal load, there is an increasing tendency for the ball to slide up the sample giving non-spherical craters [8]. There is also a potential source of error in the normal load due to the contribution to the effect of friction between the sample and ball which alters the effective weight of the ball. In the commercially marketed test system of this type [9], this potential error is reduced by using a load cell placed under the sample holding plate to measure the real normal load. Finally, it should be noted that for typical test balls, the maximum applied load that can be used is relatively small (about 0.4 N).

There is also another type of free ball machine which uses a 30 mm ball supported on grooves on two rotating shafts (Figure 3b) [10, 11]. The sample is clamped into a pivoted arm with dead weight loading applied directly above the ball. The face of the sample is pressed against the top of the ball, and the load is applied range is from 0.5 to 5 N. Again this test system variant suffers from uncertainty in the speed of the ball because of the lack of the direct drive. However, the twin shaft arrangement avoids the potential error in applied load due to friction between the ball and the test sample, and also enables higher test loads to be applied than with the inclined plane system.

2.3 DIRECTLY DRIVEN SYSTEM (FIXED BALL)

In this configuration (Figure 3c,) the ball is driven directly by clamping the ball in a split drive shaft which allows balls to be removed and replaced easily. The sample is pressed into the rotating ball from the side by test loads placed on the weight pan. This design also allows for the application of loads exceeding the mass of the ball. Test systems of this type are now also marketed within Europe [12].

2.4 RELEVANCE

There is considerable interest in these techniques for the abrasion testing of coatings. It is estimated that approximately 50 test systems of the different types described above have been set up in the last few years at a number of coating suppliers, users and research establishments. There are several reasons for this:

- The test equipment is relatively cheap to purchase or manufacture
- Test samples can be quite small as the size of the wear scar that is produced is small. This enables the technique to be used on small test coupons produced during the development of new coatings; as a technique suitable for quality control testing of coatings; and to perform tests on coated components to check the quality.
- It has the potential to be developed into an on-site test system, ie the test can be carried out in the field rather than the component having to come to the test laboratory.
- The test system seems simple and is thus attractive.
- The test system can also be used for thickness measurement.
- The test system can be used for profiling.

This latter point is particularly useful since depth scars often appear to be deep in systems with a hard coating on a soft substrate when in fact the actual loss of material be quite small with the depth of the wear scar caused by substrate deformation.

3 BASIC PRINCIPLES

Figure 1 shows the basic configuration of the ball tests. The ball is rotated against the test sample. Wear takes place to the sample and a crater is formed whose size provides a measure of the wear that as occurred. Often abrasive tests are performed by dripping abrasive slurry into the contact between the ball and the sample. Tests can be carried out limiting the duration of the test so that no perforation of the coating occurs. When performation does occur, analysis of measurements of overall crater diameter (b in Figure 1) and the diameter of the crater in the substrate (a in Figure 1) for sets of tests performed to different test durations can yield wear rates for the substrate and the coating.

3.1 TESTS WITHOUT PERFORATION

For monolithic materials, or for tests where perforation of the coating does not occur the volume V of a crater is given by

$$V = \frac{\pi b^4}{64R} \quad (1)$$

with 2b the crater diameter, and R the ball radius (for b << R)

This relationship assumes that the shape of the crater is conformal to the shape of the ball. This assumption has been shown to be true in many cases.

The Archard wear law states that the volume of wear $V = K\,SN$ where K is a constant (the wear rate), S is the sliding distance and N is the applied load. This has often been found to be true, but in some cases a strong dependence of wear rate on the number of revolutions and hence the sliding distance was found (Figure 4) [8].

However if the Archard wear law is followed, the wear rate K is described by

$$K = \frac{\pi b^4}{64R} \cdot \frac{1}{SN} \quad (2)$$

By performing tests without perforation of the coating wear rates can be measured easily for different coatings. This process is illustrated in Figure 5 where a number of experiments have been performed on a range of coatings. In Figure 5a measurements of the overall crater diameter are given. As the test duration (number of revolutions) increases the size of the crater increases. Perforation occurs for some of the coatings.

Equation 1 is used to calculate the wear rates shown in Figure 5b. Only the values for crater diameter for the craters where perforation does not occur are used. It can be seen that reasonably consistent (independent of sliding distance) wear rates are obtained for the four different coatings.

Another example is shown in Figure 6 which shows the variation in wear rate with metal content for W-C:H and Ti-C:H coatings [8].

This technique has been shown to be effective for coatings as thin as 1 μm [13]

3.2 TESTS WITH PERFORATION

When perforation of the coating occurs, the procedure that was originally developed by Rutherford and Hutchings [14,15] can be used.

A series of tests are performed with different durations (Figure 7). The inner crater diameters (a in Figure 1) and overall crater diameter (b) are both measured. Typical results are shown in Figure 8. It can be seen that there is a steady increase in the size of both diameters. Note that perforation of the coating occurs at a relatively early stage.

The analysis assumes that progress of the wear in a cratering test follows Archard's law, but this needs to be modified to take account of the perforation of the coating after a short while. This is done by using an extended Archard's law for a coating-substrate system which can then be used:

$$SN = \frac{1}{K_c} V_c + \frac{1}{K_s} V_s \qquad (3)$$

with K_c and K_s are the wear coefficients of the coating and substrate respectively, V_c and V_s the measured wear volumes and SN the sliding distance multiplied by the applied load.

There are different ways of implementing equation (3). It could be solved using a multiple least squares approach. The wear coefficients K_c and K_s are then considered both as unknowns. However, the equation is rather unstable, because of the relationship between V_c and V_s.

A better methodology is to rewrite the equation (3) as a linear function. Conventionally two forms are used. The first one is:

$$\frac{SN}{V_t} = \left(\frac{1}{K_c} - \frac{1}{K_s}\right)\frac{V_c}{V_t} + \frac{1}{K_s} \qquad (4)$$

where V_t is the total worn volume. The formula is more stable when $\frac{V_c}{V_t} < 0.5$. Figure 9a [16] shows schematically the linear relationship and the direction in which datapoints are measured in the test. As long as there is no perforation $\frac{V_c}{V_t}$ is equal to 1.

Formula (4) can be simplified by using an estimation of the wear cap volume and by introducing the measured thickness t of the coating. This equation was derived by Rutherford and Hutchings [14]:

$$SN\left(\frac{64R}{\pi b^4}\right) = \left(\frac{1}{K_c} - \frac{1}{K_s}\right)\left(\frac{16Rt}{b^2} - \frac{64R^2t^2}{b^4}\right) + \frac{1}{K_s} \qquad (5)$$

The coating thickness, t, can be calculated from the same micro-abrasion test or can be measured separately.

A second way of rewriting equation (3) is (see also Figure 9b)

$$\frac{SN}{V_t} = \left(\frac{1}{K_s} - \frac{1}{K_c}\right)\frac{V_s}{V_t} + \frac{1}{K_c} \qquad (6)$$

The simplified version of this equation is (see Rutherford and Hutchings [14])

$$SN\left(\frac{64R}{\pi b^4}\right) = \left(\frac{1}{K_s} - \frac{1}{K_c}\right)\left(1 - \frac{16Rt}{b^2} + \frac{64R^2t^2}{b^4}\right) + \frac{1}{K_c} \qquad (7)$$

Other ways to elaborate equation (3) are obtained by dividing by either the wear volume in the coating or in the substrate (the linear relationships described are shown schematically as Figures 9c and 9d):

$$\frac{SN}{V_c} = \frac{1}{K_c}\frac{V_t}{V_c} + \left(\frac{1}{K_c} - \frac{1}{K_s}\right) \quad (8)$$

$$\frac{SN}{V_s} = \frac{1}{K_c}\frac{V_t}{V_s} + \left(\frac{1}{K_s} - \frac{1}{K_c}\right) \quad (9)$$

Equation (9) does not seem very useful, since the term V_t/V_s is large when the crater is still mainly in the coating and only with a small crater in the substrate. The equation can be used successfully for the K_c determination however if a least squares method with weighting factors is used, based on the accuracy of the measurement of the wear volume.

An example of the application of the analysis is given in Figure 10 where equation 5 has been applied to the analysis of the results from Figure 8. In this case a very good linear fit has been achieved leading to confidence in the calculated values of the wear rates for the coating and the substrate.

3.3 SLIDING WEAR TESTING

Recently the ball cratering test has been modified to give the capability for performing sliding wear tests (Figure 11) [17]. The test system has been modified by adding strain-gauged leaf springs to enable the measurement of frictional force generated at the contact. A displacement transducer is also fitted to measure the movement of the sample towards the ball as the sample wears.

The wear scars formed in a test between a steel ball and TiN coated tool steel sample are shown in Figure 12. A large volume of brown debris was formed on the coated sample. The brown colour of the debris indicates that the debris is likely to be iron oxide. This is confirmed by the brown colour of the scar on the ball. When the scar is cleaned to remove debris, reduced wear at the centre of the scar becomes apparent[†] (Figure 13).

Typical friction and wear displacement results are shown in Figure 14. In this test the friction coefficient is high at about 1, and subject to periods of highly variable friction (shown by the high standard deviation in the friction values at certain points. The wear displacement steadily increases as the test proceeds until a final average displacement of about 4 μm was observed.

4 SECTIONING

Ball cratering can also be used for the more traditional roles of forming taper sections. This can be seen in Figure 15 that shows a crater through a multilayered coating. The structure of the coating is clearly shown at the edge of the crater.

[†] see later section on load effects.

If the ball crater test system is being used to carry out sectioning rather than to perform a wear test, it is important to optimise the test conditions so that a smooth crater surface is obtained. This is normally achieved by using low applied loads and fine abrasives.

Precise positioning can be achieved which enables the technique to be used as a method of measuring the profile of wear tracks from other types of wear tests such as pin-on-disc wear tests. This can give a very accurate measure of wear, and also has the advantage that sub-surface deformation under the wear track can be detected. This is important when wear tests are carried out on wear resistant coatings such as DLC on softer substrates where an apparent wear track is formed which is shown to be due entirely to sub-surface deformation (Figure 16) [18].

5 PARAMETERS AFFECTING RESULTS

There are a large number of parameters that affect the results of ball cratering tests. These include:

- the abrasive material
- the abrasive size
- the abrasive shape
- the abrasive loading
- the type of suspension fluid
- the load
- the speed
- the ball material
- the ball surface condition.

5.1 ABRASIVE

The abrasive material is clearly important. The main reason is the hardness of the abrasive, and in general, the harder the abrasive, the higher the wear rate. However, it is important to realize that it is the relative ratio of hardness between the abrasive, the ball material and the sample that is important.

The size of the abrasive is also important. It has been shown from consideration of the frictional forces that act between the test surfaces and the abrasive particles that there will be upper limit of abrasive which can be drawn into the interface between the ball and the sample [13]. Clearly if no abrasive is present at the interface, the wear mechanism changes radically. For the size of balls that are normally used (25 mm diameter), this limit will be in the range 10-20 μm diameter. This is the main reason that this test is most appropriate (for abrasion testing) for use with fine abrasives. Typically abrasives less than about 5 μm diameter are used.

Under some conditions, craters made with coarse abrasives can be difficult to measure as the edge of the craters are obscured by grooving from the abrasive. When this occurs, the use of finer abrasive can give better crater definition (Figure 17) [8].

As with all abrasive tests, the shape of the abrasive is important. Abrasives with more angular shapes will give higher loading when they are pressed and moved against the sample. For this reason abrasive damage and wear are likely to be higher for more angular shaped abrasive particles.

5.2 ABRASIVE LOADING AND LOAD

The effect of applied load and the concentration of abrasive in the slurry are linked. As the load is increased there is a transition from a three body rolling wear mechanism to a two body grooving mechanism. Conversely, as the volume fraction of abrasive is increased, there is transition from two-body grooving to three-body rolling. These transitions can best be expressed [19] by a wear mechanism map (Figure 18). Typical micrographs of the surfaces of samples produced in these different regimes are given in Figure 19.

The gross appearance of craters tested in the two body grooving regime are typically shiny in appearance (Figures 19b and 20) with a regular array of grooves over the surface. By contrast, surfaces of samples tested in the rolling regime are dull in appearance (Figure 19a) with much more random damage.

The slurry concentration also affects the magnitude of wear that occurs, with higher wear in the rolling wear regime at higher slurry concentrations [19] (Figure 21).

When the load is increased further, the phenomena of ridging occurs (Figure 22). Little or no wear occurs at the centre of the scar because of blocking of abrasive ingress at the centre of the contact resulting from the high Hertzian contact pressures at the centre of the contact. This prevents abrasive from entering this contact region and thus reduces or eliminates abrasive wear in the centre of the scar. The ridging prevents further increases in wear with increasing load above a critical load value (Figure 23).

As well as the phenomenon of ridging, there is evidence that at high loads abrasive can also be embedded into the sample surface leading to erroneous results (Figure 24) [8].

5.3 SUSPENSION FLUID

Clearly, if the composition of the slurry suspension fluid promotes corrosion or chemical reaction with the sample, a synergistic effect of variation of the wear rate is likely to occur. Although there is some evidence that the physical properties of the fluid such as viscosity may have an impact on results [8] for high viscosity fluids such as glycerine, for many practical suspension fluids (eg water), the speed of relative motion between the ball and the sample is sufficiently low that hydrodynamic lubrication effects are not important.

There may be lubrication effects due to changes in the way the suspension fluid lubricates the contacts between the ball, abrasive particle and sample, but there is currently no clear evidence for this.

There is conflicting evidence over the effect of suspension dosage. Some workers suggest that as long as there is always sufficient suspension at the wear interface there will be no effect on results, whilst others report a high influence and state the need to dose the slurry precisely [8].

5.4 SLIDING SPEED

The wear volume (at constant sliding distance) is largely independent of sliding speed, but increases somewhat for very low speeds (Figure 25) [10].

For the free ball machine, the tendency of the ball to slip on the shaft increases as the speed increases. This can lead to an apparent decrease in wear as the ball increases (Figure 26) [8].

5.5 BALL MATERIAL

There are two effects of changing the ball material; both due to the changes in the relative hardness. Thus a softer ball will encourage embedding of abrasive particles into the ball, reducing separation between the surfaces and enhancing grooving wear.

If very soft balls are used, the normal assumption in the calculation of wear volumes that the wear scar is conformal to the unstressed shape of the ball may not be true. The ball deforms under the applied load so that the contact area becomes much larger than would be otherwise expected. This makes analysis of test results much more complex.

Unless there are special reasons for using other materials, most users use hardened steel balls.

5.6 SURFACE BALL CONDITION

The condition of the test ball has been shown to have a major effect on the wear that occurs. As balls are used in tests, they become roughened through abrasion and potentially corrosive damage.

In experiments where the wear displacement was measured as a way of monitoring wear on-line, the wear obtained with used balls was compared with the wear obtained with new balls (27). It was found that the wear displacement for the worn balls was more reproducible than with the new ball. This was confirmed to be due to a lack of entrapment of abrasive particles with the new balls. As the test proceeds, and the ball gradually roughens, abrasive becomes entrapped in an irregular random fashion. With the rougher used balls entrapment occurs almost immediately the test starts.

Although surface treatments have been developed for the balls [20] to eliminate the variability introduced by this effect, perhaps a better procedure is to condition new balls by carrying out a "running in" procedure on the new balls on a sacrificial part of the sample.

As well as reducing variability in results, the use of treated or used balls increases the wear that is observed (Figure 28). However, as wear to the test ball continues a flat band can be worn on the ball giving erroneous results. It is therefore important to ensure measure the ball at regular intervals and replace it if it becomes too worn.

6 FACTORS AFFECTING MEASUREMENTS

Factors that affect measurement are:

- the difficulty in resolving the edges of craters
- the method of scar size measurements
- the fact that non-perfect crater slops are often seen in tests
- the theory for analysing results may not be appropriate for all materials and test conditions.

6.1 ILL DEFINED CRATER EDGES

Often there can be difficulties in defining the edges of craters. Figure 29 shows the edge of a crater made in a TiN coating on tool steel. Grooving wear took place in this test, but some of the grooves were so deep that it made measurement of the inner crater diameter impossible in this case (also see Figure 17). This Figure (29) also shows that there is a region of scuffing that has occurred around the edge of the crater. This scuffing can cause difficulties in determining the real edge of the crater. Thus in Figure 30, optical microscopy can be seen to overestimate the size of the craters by comparison to direct profilometric measurement of wear volume [13] (look at the gap between the two craters when comparing the two measurement methods). A similar result can be seen in Figure 31 [8] where the wear rate calculated from optical measurements is larger than that calculated from profilometry measurements.

6.2 DIFFERENT MEASUREMENT METHODS

The different measurements that have been used for crater size measurement are:

- optical microscopy through image analysis or travelling microscopy
- profilometry through interference microscopy, laser optical techniques, or mechanical probe devices.

The use of profilometry sometimes overcomes the difficulties mentioned in the last section, but clearly the boundary between the portion of the crater in the coating, and the portion in the substrate cannot be distinguished by this method, as profilometry can only be used for testing where perforation does not occur.

6.3 REPRODUCIBILITY

The ball cratering instrument has been tested using standard wear protective coatings e.g. DLC, W-C:H and TiN. The results for W-C:H and TiN are shown in Figure 32 [8]. The

sliding distance (number of revolutions) has been adjusted in a way that the wear process is limited to a depth of 1 μm, where the wear properties of the coating could be measured without influence of the substrate or interlayer. The measurements show high reproducibility of the wear depth measurement with a standard deviation of less than 5%.

6.4 COMPARISON BETWEEN PERFORATING TESTS AND NON-PERFORATING TESTS

It is useful to compare the two modes of use of the ball cratering test. Clearly for thick coatings (more than 10 μm in thickness), the non-perforating test will be most useful as perforation for these coatings will take a long time. In this situation, good measurement accuracy can be achieved without the need to make the assumptions that lie behind the analysis for the perforating test that may not be valid in all cases. For thin coatings (less than 1 μm) the coatings are perforated very quickly, and the only possible route is the use of the perforating test is the only option. However, as the coating becomes thinner, it becomes increasingly difficult to measure and differentiate the relative sizes of the inner and outer craters so accuracy is a concern.

Between these two limits either type of test and the relative merits of both types of test will vary with the materials that are being tested.

A systematic comparison between perforating and non-perforating tests has not yet been made; this is one of the expected outcomes of the CRATER EU project.

7 ACKNOWLEDGEMENTS

The author would like to acknowledge the support of the EU through the Framework V Growth contract GRD1-2000-25020 for the work reported here.

REFERENCES

1) E Santner, D Klaffke, G Meier zu Kocker, Comprehensive tribological characterisation of thin TiN based coatings,Wear, 190(1995)204-211
2) H Ronkainen, K Holmberg, K Fancey and A Matthews, B Mathes and E Broszeit, Surface and Coatings Technology, 43-44(1990)888-897
3) H Vetters et al, Development and Validation of Test Methods for Thin Hard Coatings (FASTE), Final report, EU Contract, MAT1-CT 940045
4) E A Almond, L A Lay, M G Gee. Comparison of Sliding and Abrasive Wear Mechanisms for Cemented Carbides and Ceramics, Proceedings of 2nd International Conference on the Science of Hard Materials, Institute of Physics Conference Series No 75: p919, Adam Hilger, 1986
5) S J Bull, D S Rickerby, A Matthews, A Leyland, A R Pace and J Valli, Surf Coat Technol, 36(1988)503
6) R Gahlin, M Larssen, P Hedenquist, S Jacobson & S Hogmark. The crater grinder method as a means for coating wear evaluation - state of the art, Surface & Coatings Technology.
7) J von Stebut, Private Communication, October 2001
8) R Bethke, K Schiffmann, Ball Cratering Wear Test: Review of the State of the Art, Fraunhofer Institut fur Schicht und Oberflachentechnik, Braunschweig, May 2001
9) Calowear Test System, CSEM, Neuchatel, Switzerland.
10) Y Gachon, Industrial Experience from HEF R&D on Abrasion Testing by Ball Cratering System, HEF R&D, May 2001
11) Gencoa Ball Cratering Test System,
12) TE 66 Test System, Plint and Partners, Wokingham UK
13) D N Allsop, Abrasive wear of bulk materials and hard coatings, phD thesis, University of Cambridge, 1999
14) K L Rutherford, I M Hutchings. A micro-abrasive wear test, with particular application to coated systems. Surface & Coatings Technology, 79 (1996) 231-239.
15) K L Rutherford, I M Hutchings, Theory and application of a micro-scale abrasive wear test, Journal of Testing and Evaluation, 25(1997)250-260
16) K Van Acker, Private Communication, May 2001
17) M G Gee and M J Wicks, Ball Crater Testing for the Measurement of the Dry Unlubricated Sliding Wear of Wear Resistant Coatings, Surface Coatings Technology, 133-134(2000)376-382
18) Teer BC-1 Ball Crater Device User Guide
19) R I Trezona et al, D N Allsopp, I M Hutchings, Transitions between two-body and three-body abrasive wear: influence of test conditions in the microscale abrasive wear test, Wear 225-229 (1999) 205-214.
20) D N Allsop, R I Trezona and I M Hutchings, The effect of ball surface condition in the micro-abrasive wear test, Tribology Letters, 5(1998)259-264

FIGURES

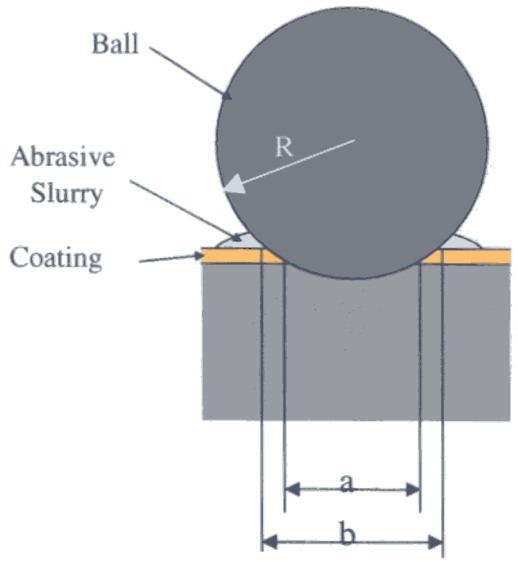

Figure 1 Principle of Test

a)

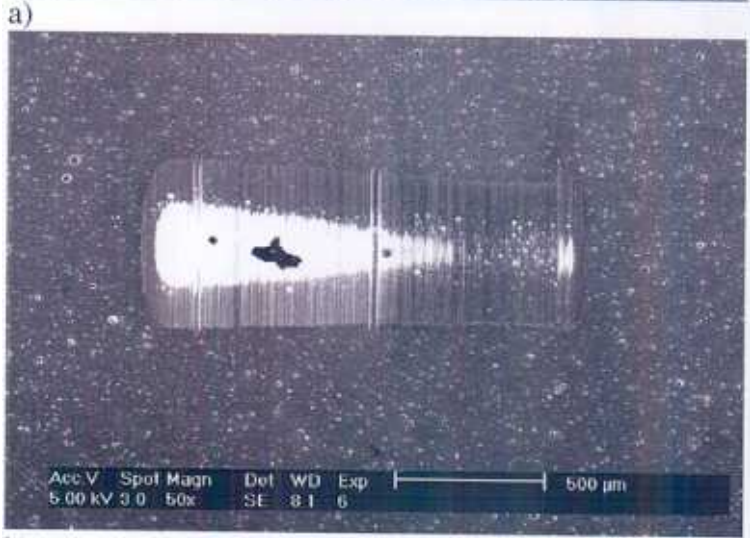

b)

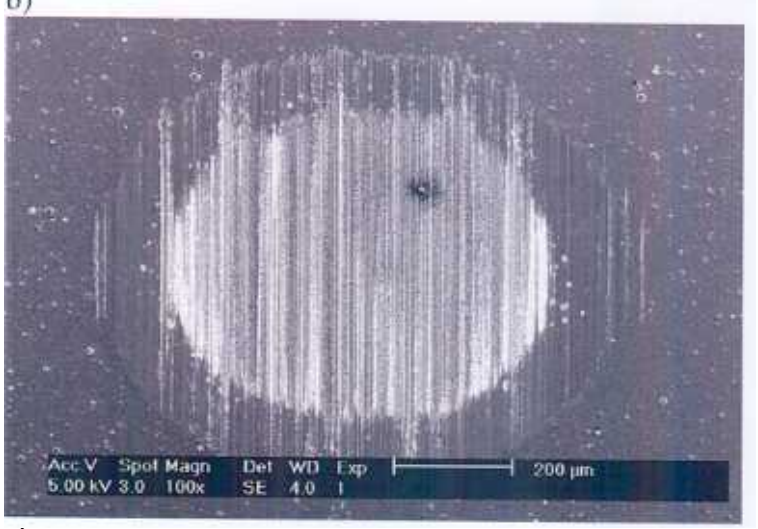

c)

Figure 2, Experiments with rotating brass wheel pressed against non-rotating sample with 1 µm diamond paste, a) new wheel for duration of 30 minutes, b) new wheel for duration of 100 minutes, c) worn wheel for duration of 70 minutes

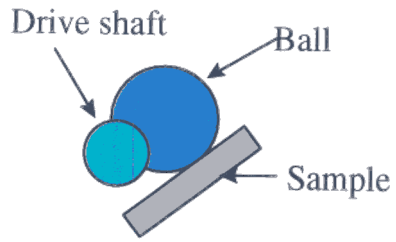

a)

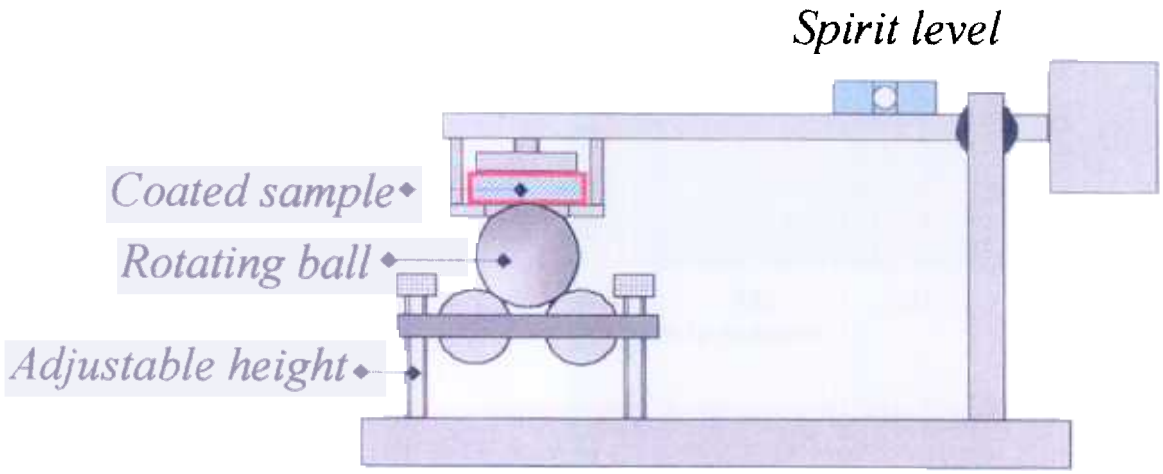

b)

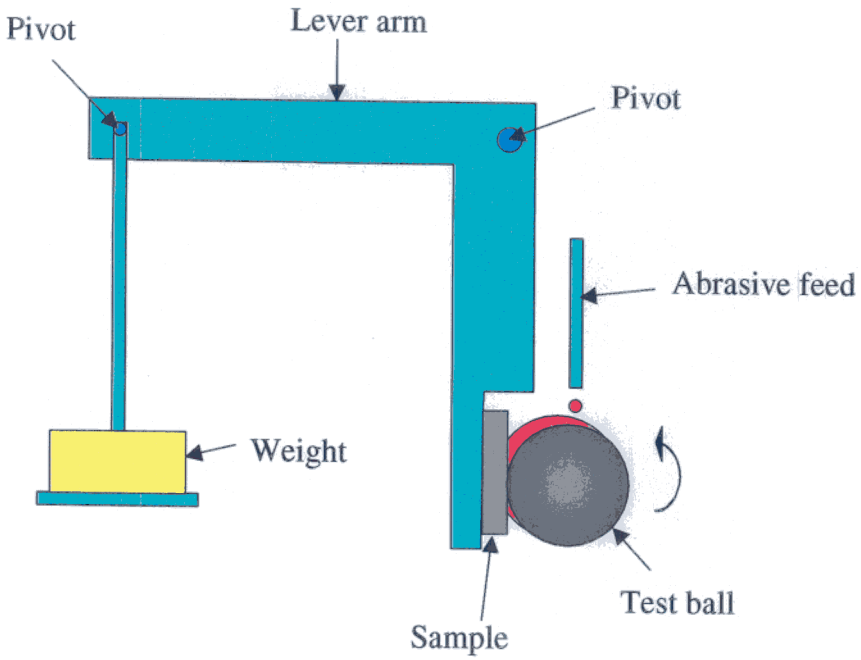

c)

Figure 3 Different test systems, a) free ball-single shaft, b) free ball-two shaft, c) fixed ball.

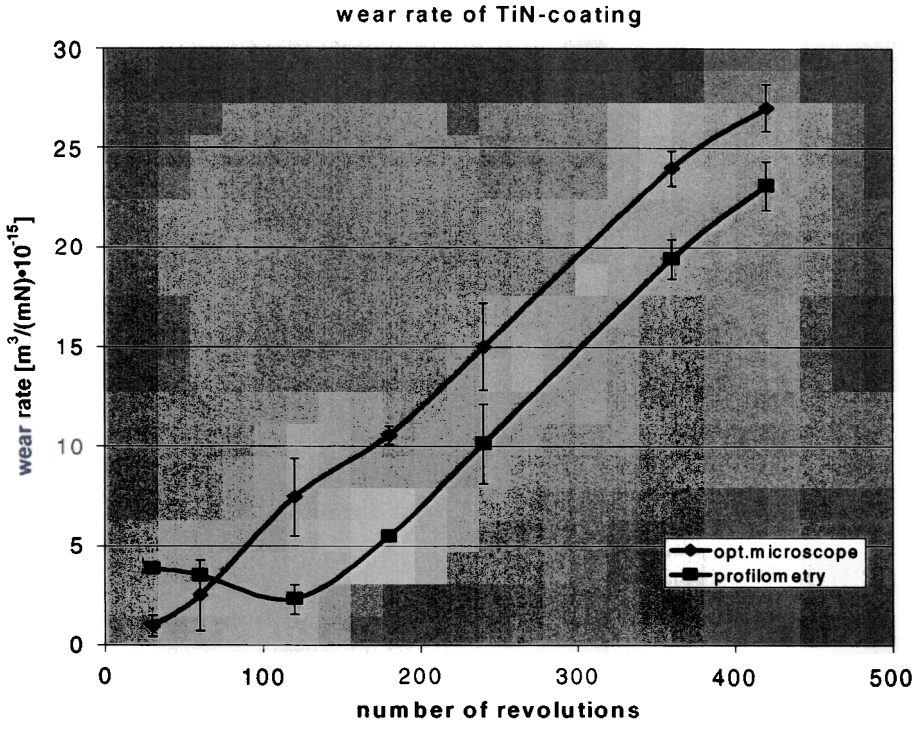

Figure 4 Wear rate of 3 μm thick TiN coating on steel. 1 μm alumina in glycerine slurry, 30 mm steel ball, 0.43 N load, 57 % RH, free ball-single shaft system [8].

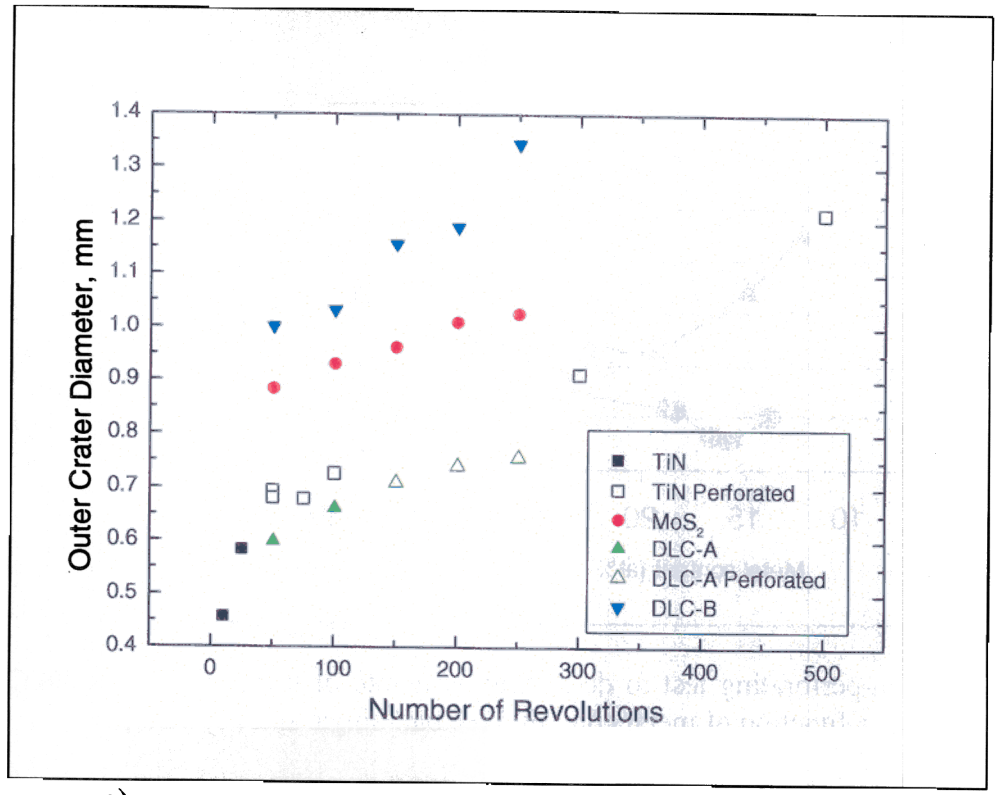

a)

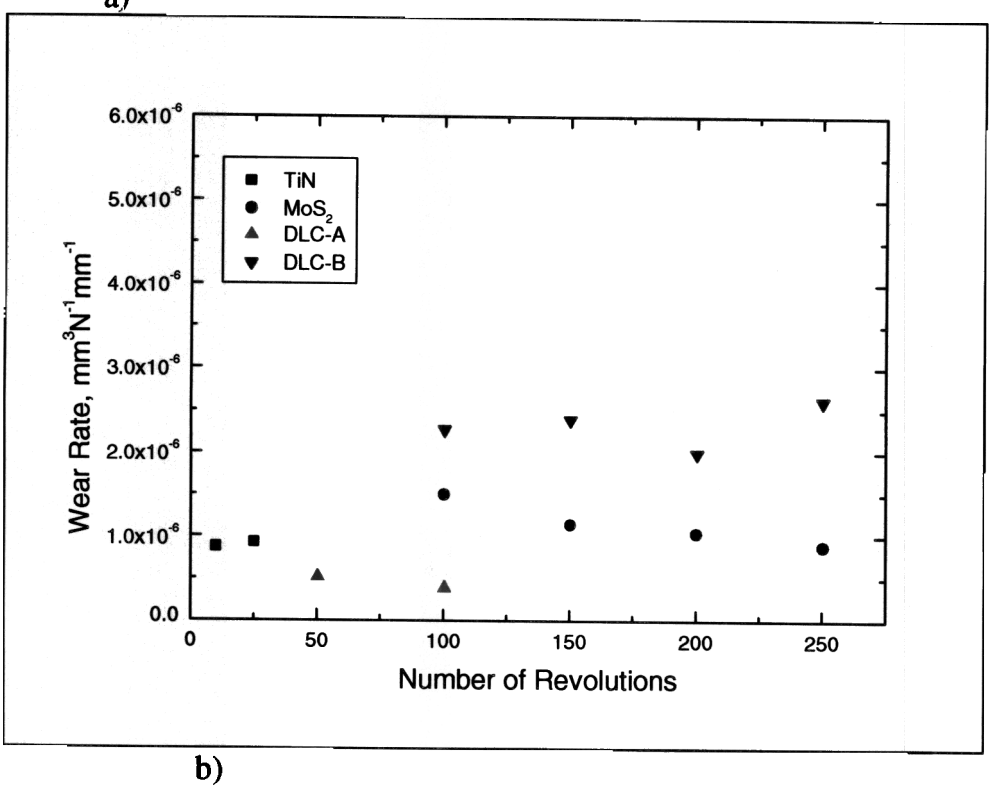

b)

Figure 5 Tests performed on range of coated samples, a) increase in overall crater diameter with increased test duration, b) calculated wear rates from non-perforated craters.

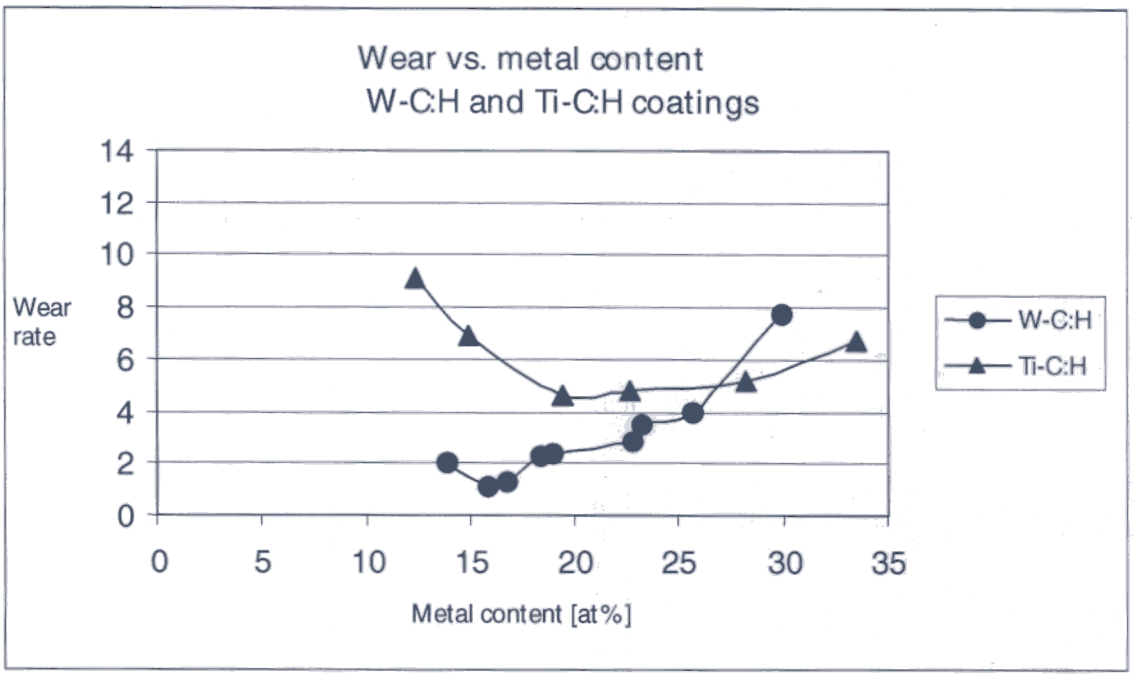

Figure 6 Use of non-perforating test to determine wear rate of metal containing DLC coatings as a function of metal content. Free ball-single shaft system [8].

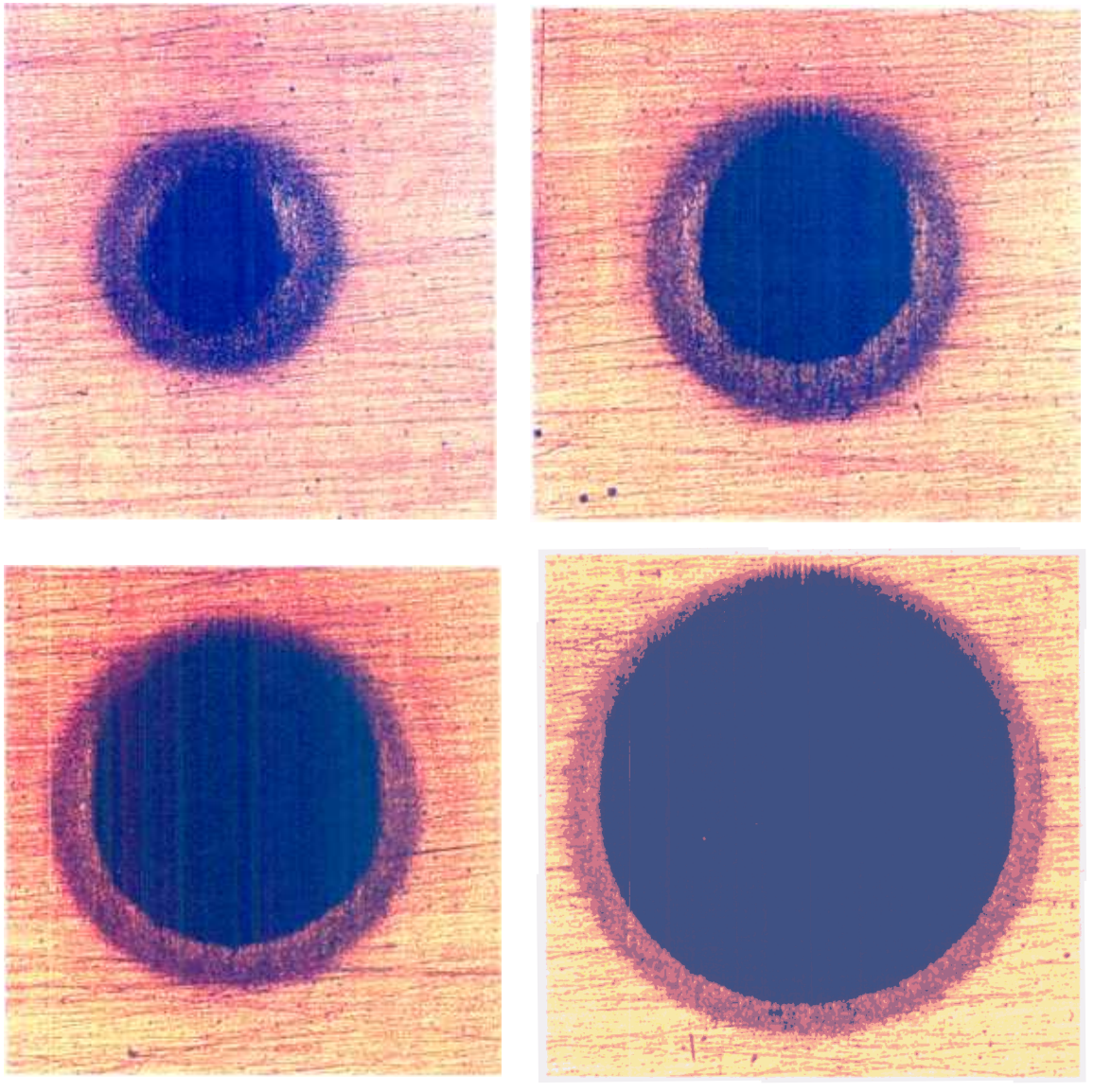

Figure 7 Craters produced by tests of increasing duration on TiN coated tool steel sample.

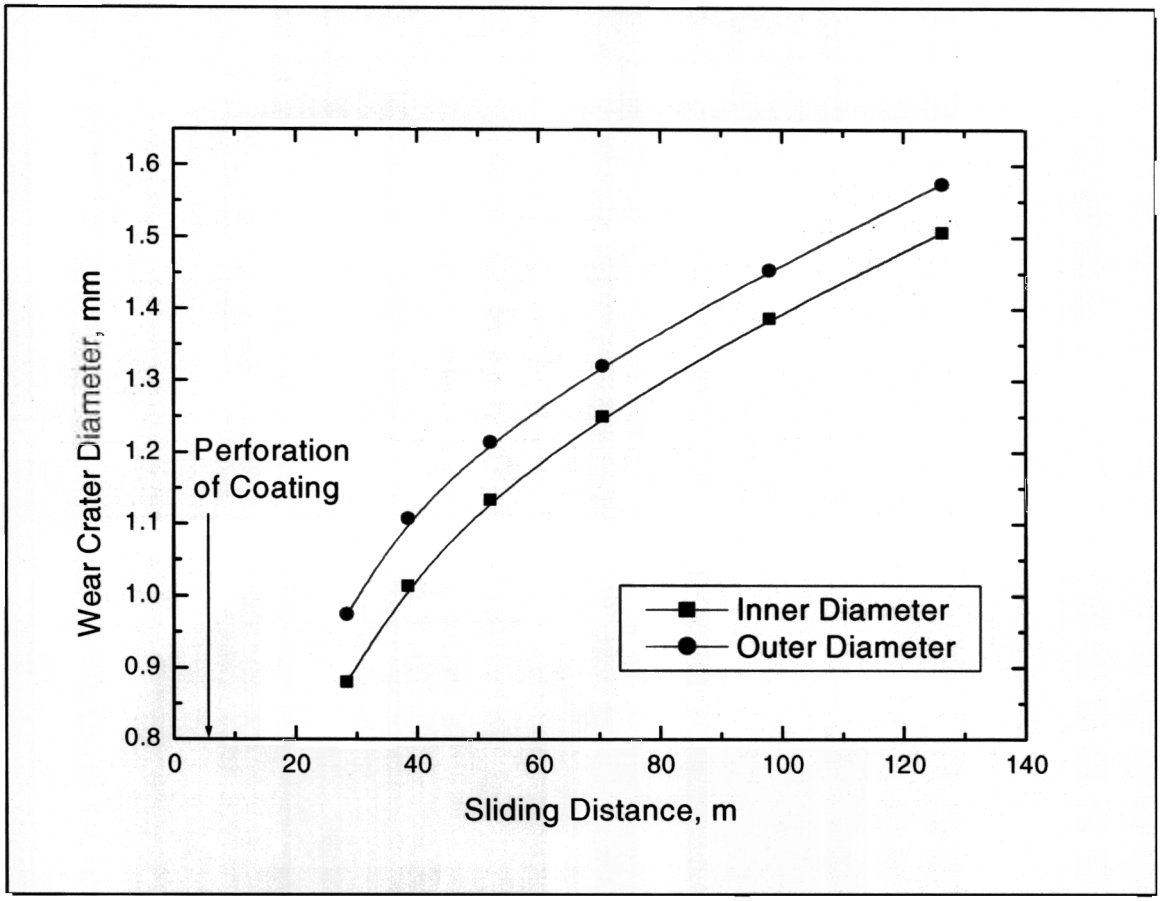

Figure 8 Measurements of crater diameter for series of tests on TiN coated steel sample. Rutherford & Hutchings [15].

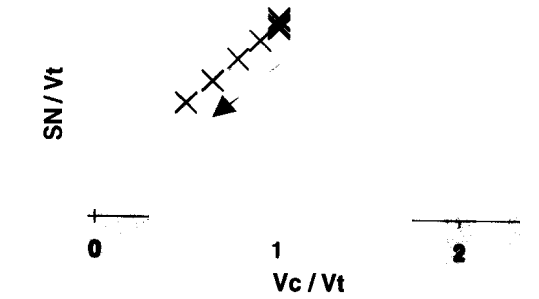

a)

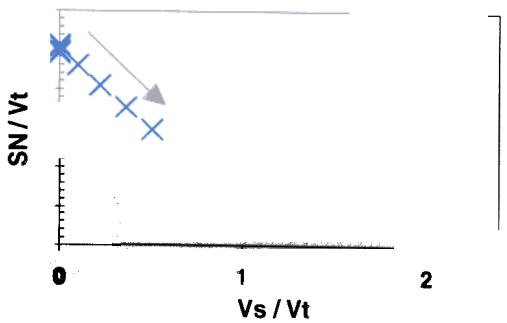

b)

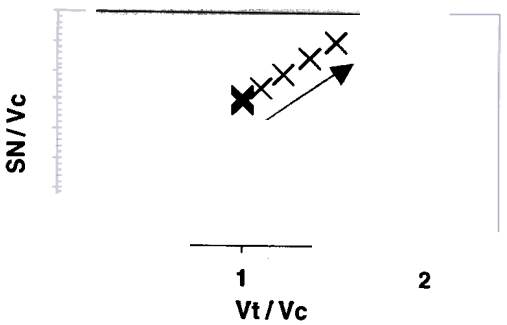

c)

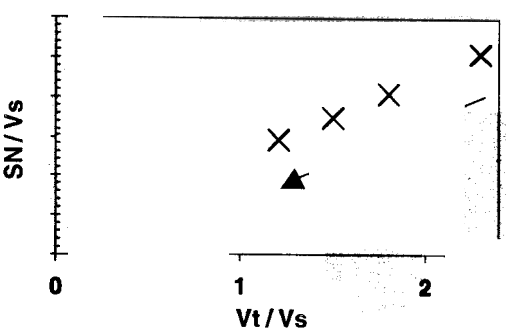

d)

Figure 9 Schematic diagrams showing linear relationships expressed in a) equation 4, b) equation 6, c) equation 8, d) equation 9 [16].

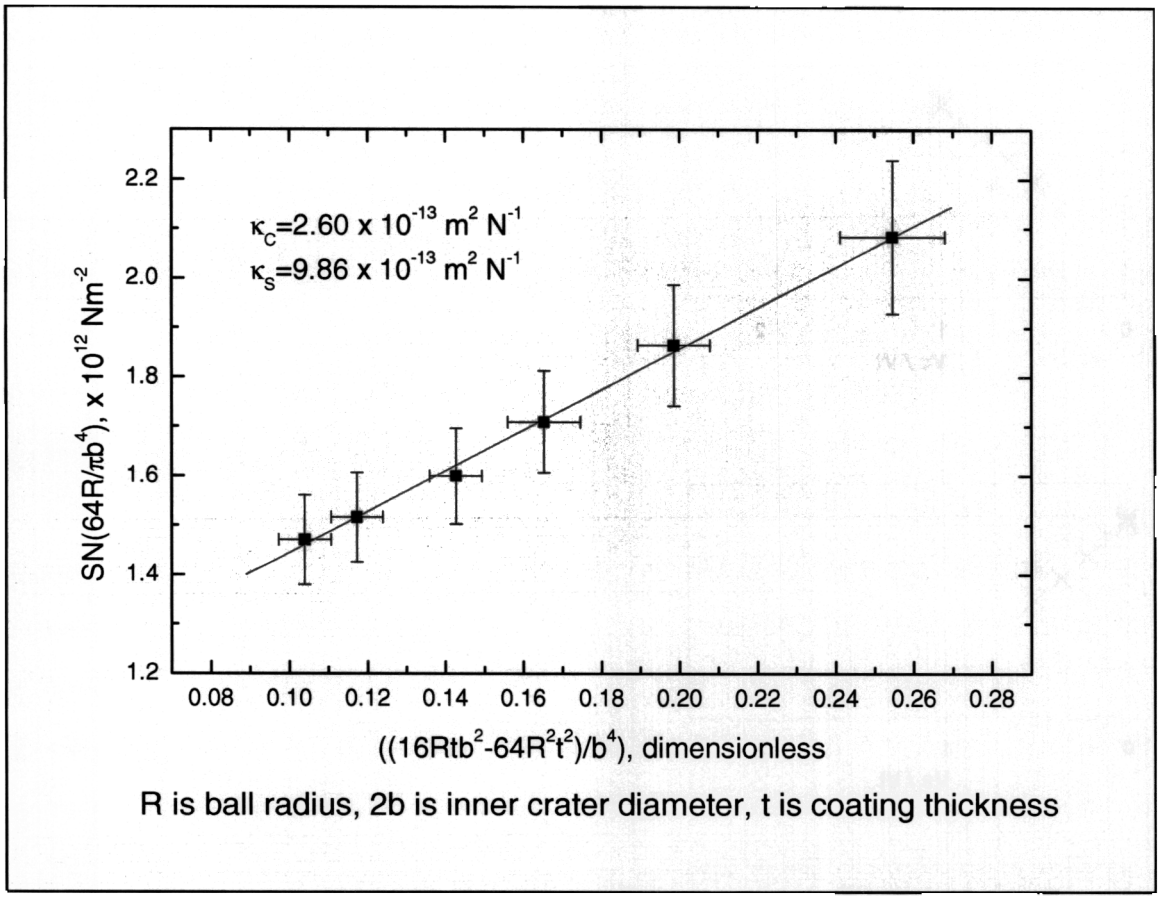

Figure 10 Analysis of ball cratering results of set of tests on TiN coated steel resulting in calculation of wear rates for steel and coating. From Rutherford & Hutchings [15].

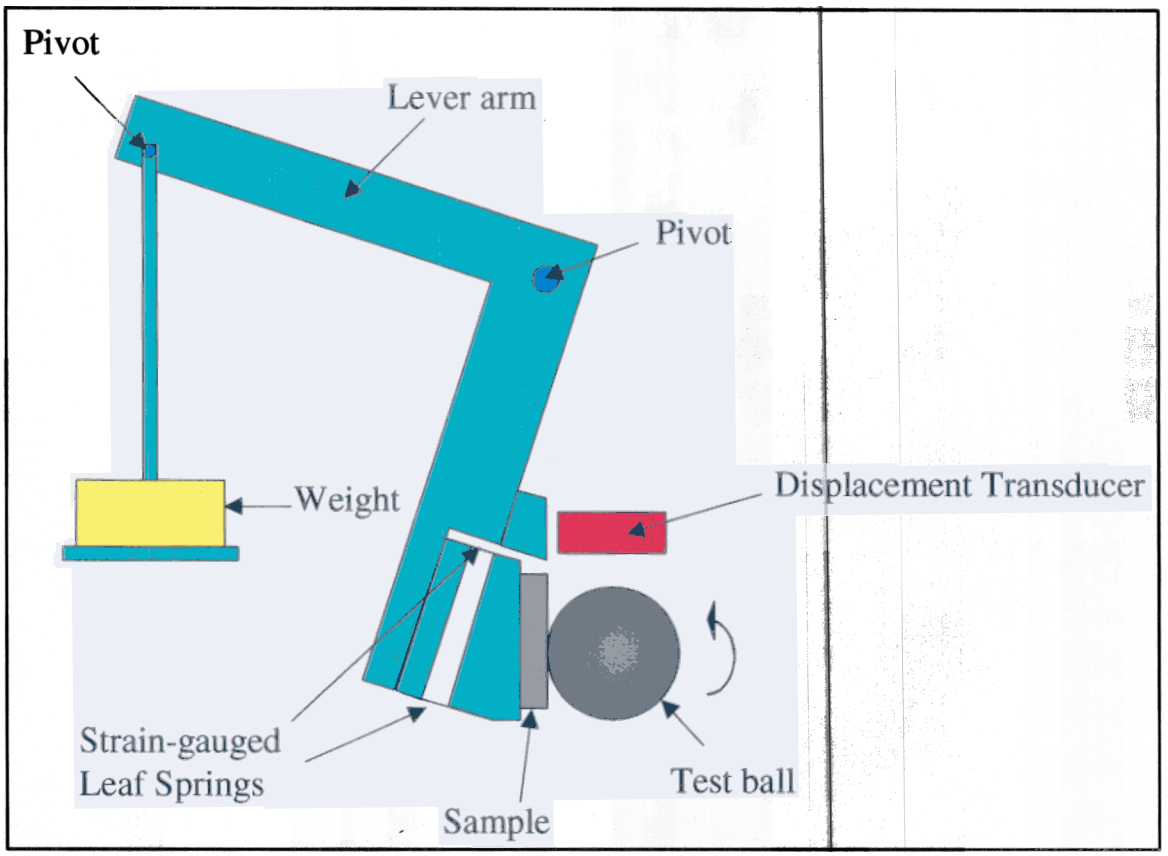

Figure 1 Modification of ball cratering tests to add friction measurement capability for sliding wear tests.

a)

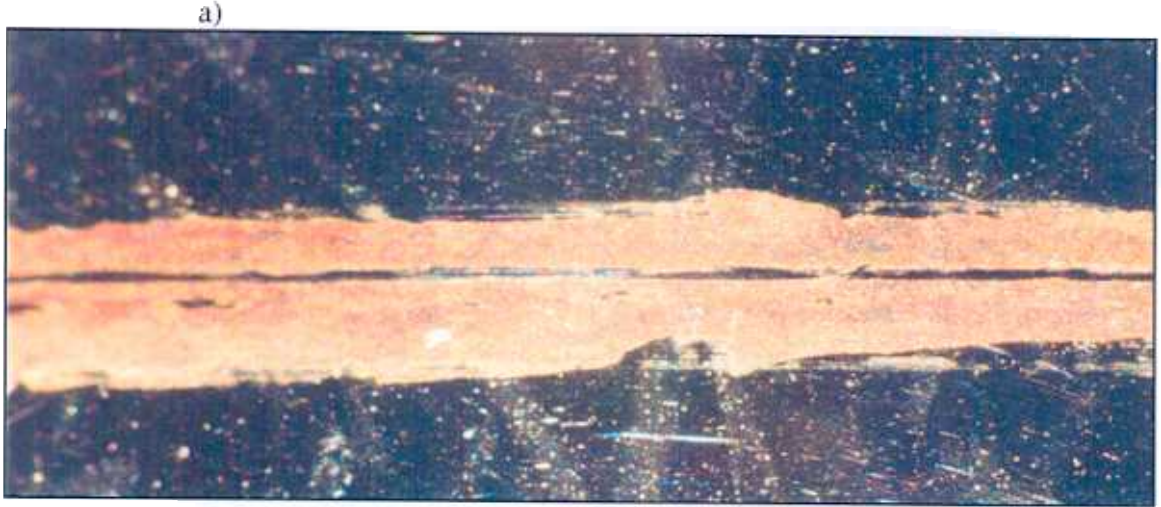

b)

Figure 12 Wear scars from dry ball cratering sliding wear tests on TiN coated steel sample, a) crater on sample, b) track on ball.

Figure 13 Cleaned wear scar from dry ball cratering sliding wear tests on TiN coated steel sample showing ridging.

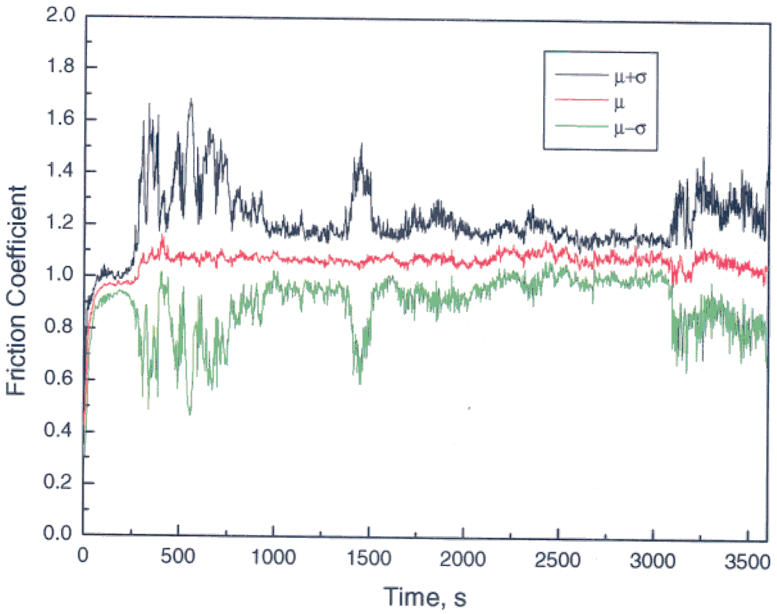

a)

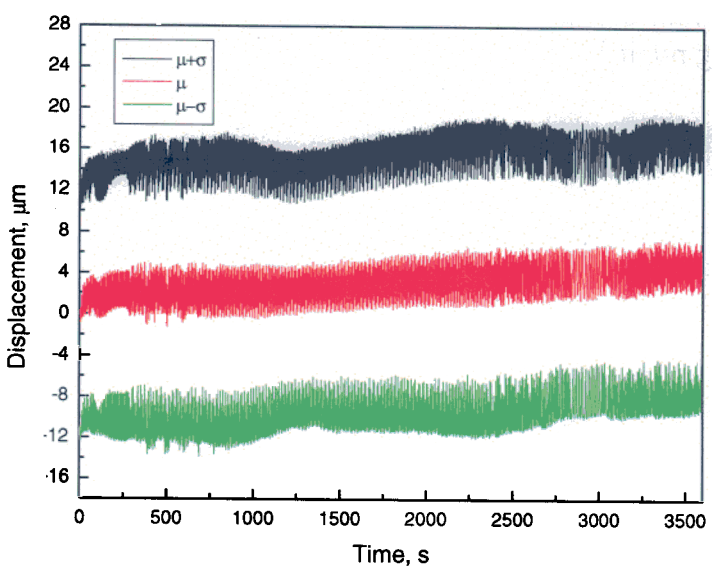

b)

Figure 14 Results of on-line measurements of friction coefficient and wear displacement for a test with a steel ball and TiAlN coated tool steel sample with an applied load of 4.7 N, a) friction coefficient, b) wear displacement.

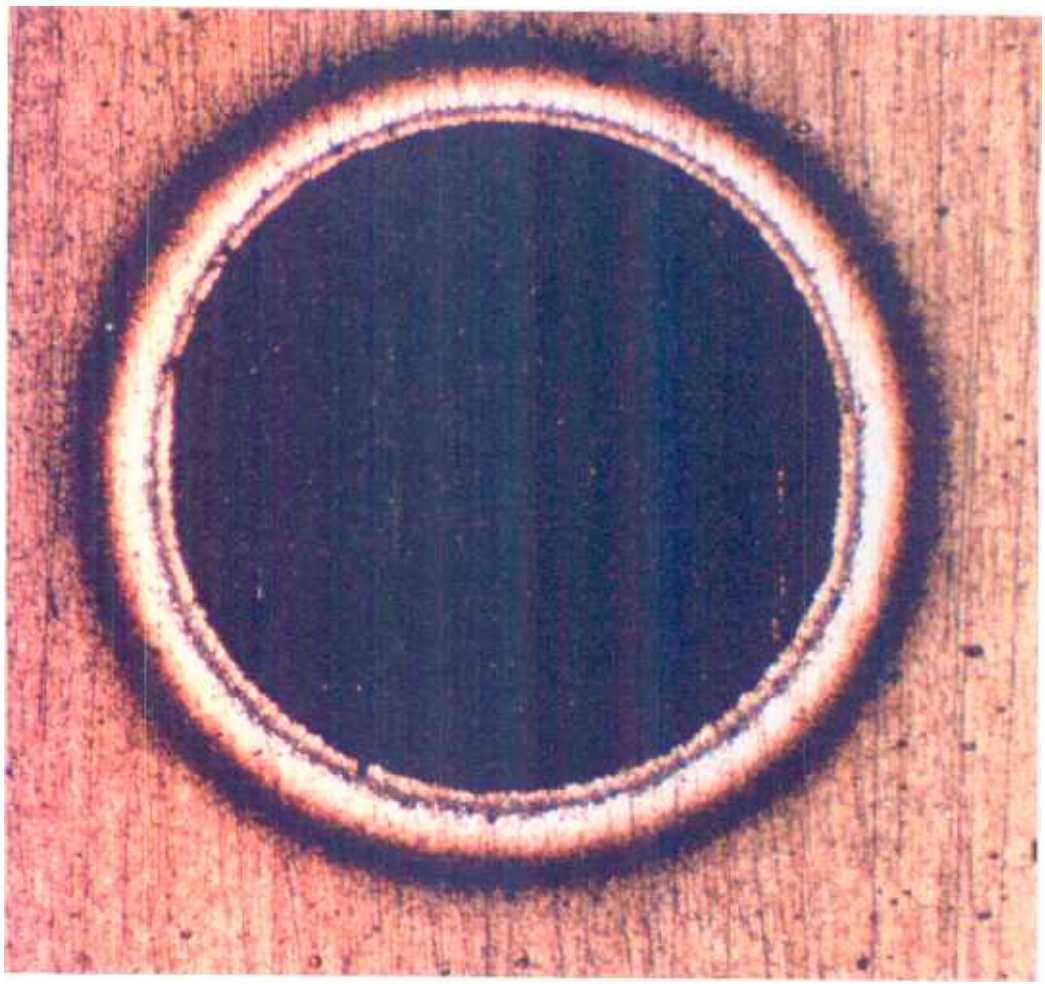

Figure 15 Ball crater showing how techniques can be used to investigate structure of coatings.

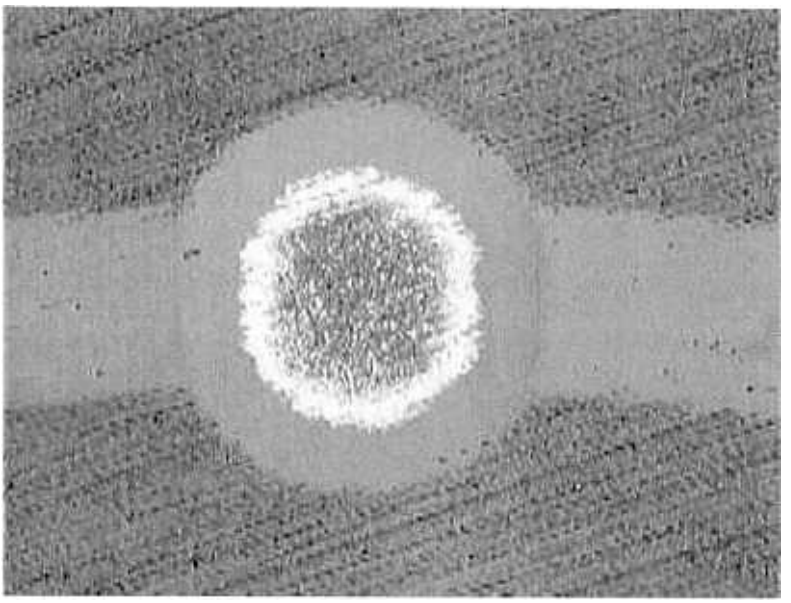

a)

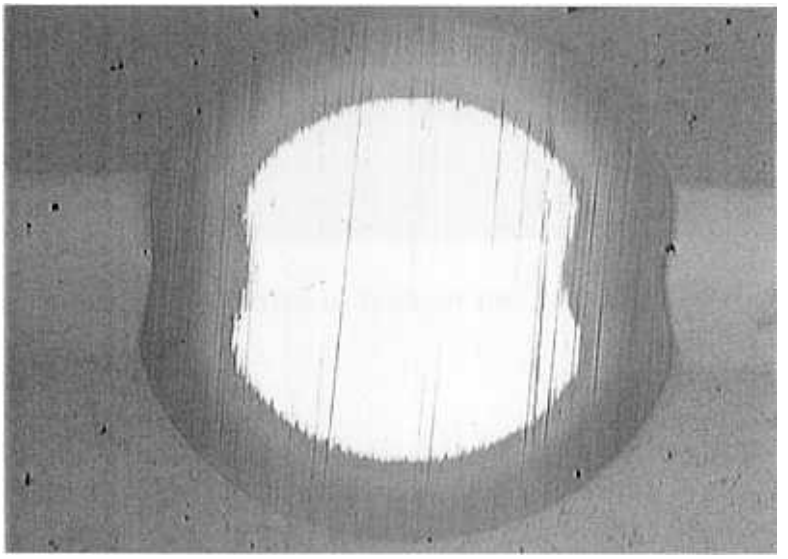

b)

Figure 16 Examples of use of ball cratering for taper sectioning, a) pin-on-disc wear track, b) apparent wear track showing clear plastic deformation of substrate under track.

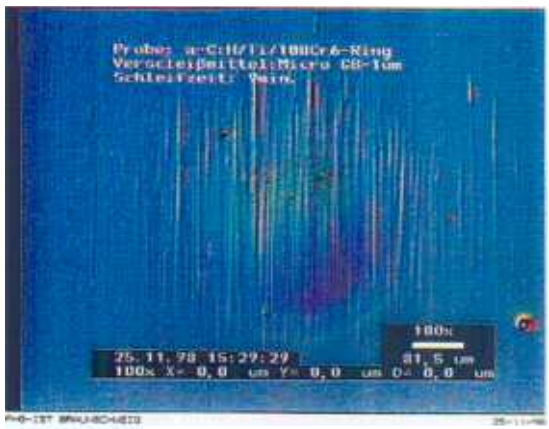

a)

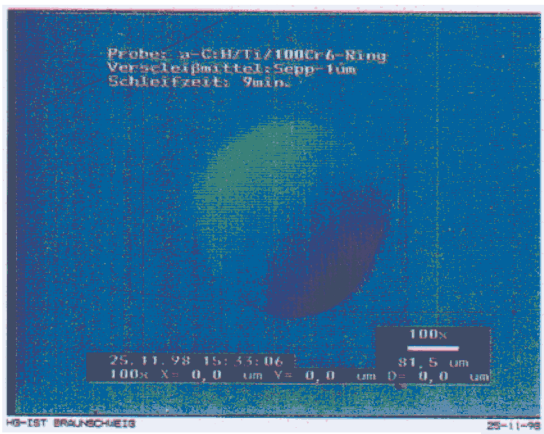

b)

Figure 17 Effect of abrasive size on crater, a) deep grooving from coarse abrasive b) well defined crater from fine abrasive [8].

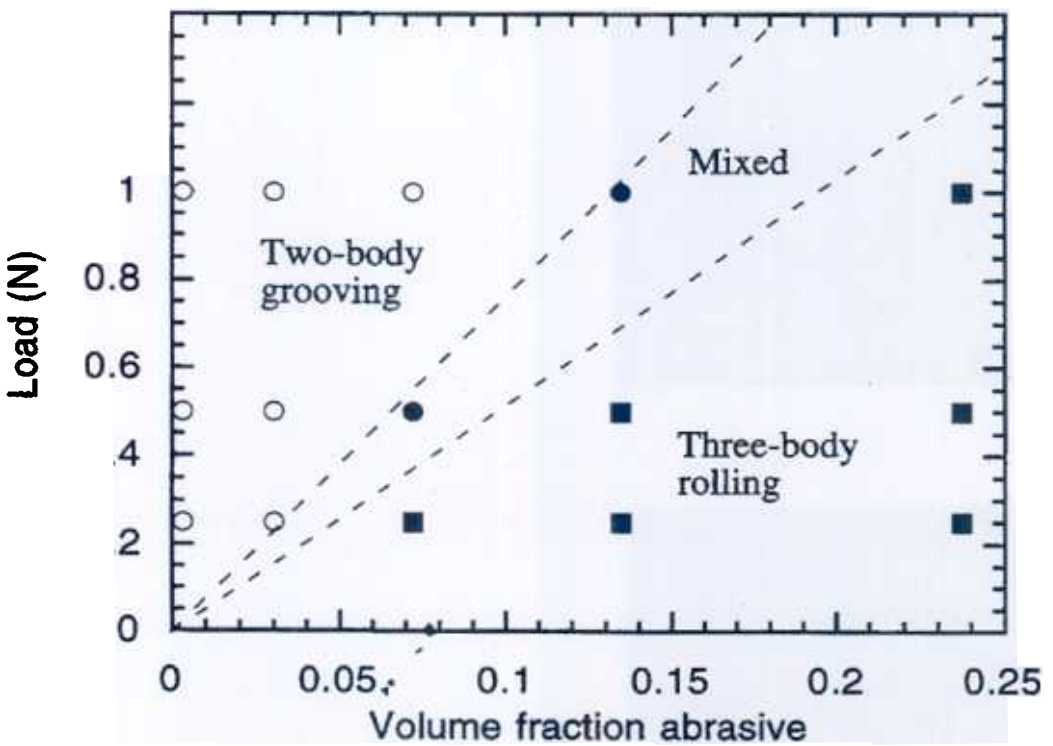

Figure 18 Ball cratering wear mechanism map for tool steel sample with SiC abrasive, ref [19]

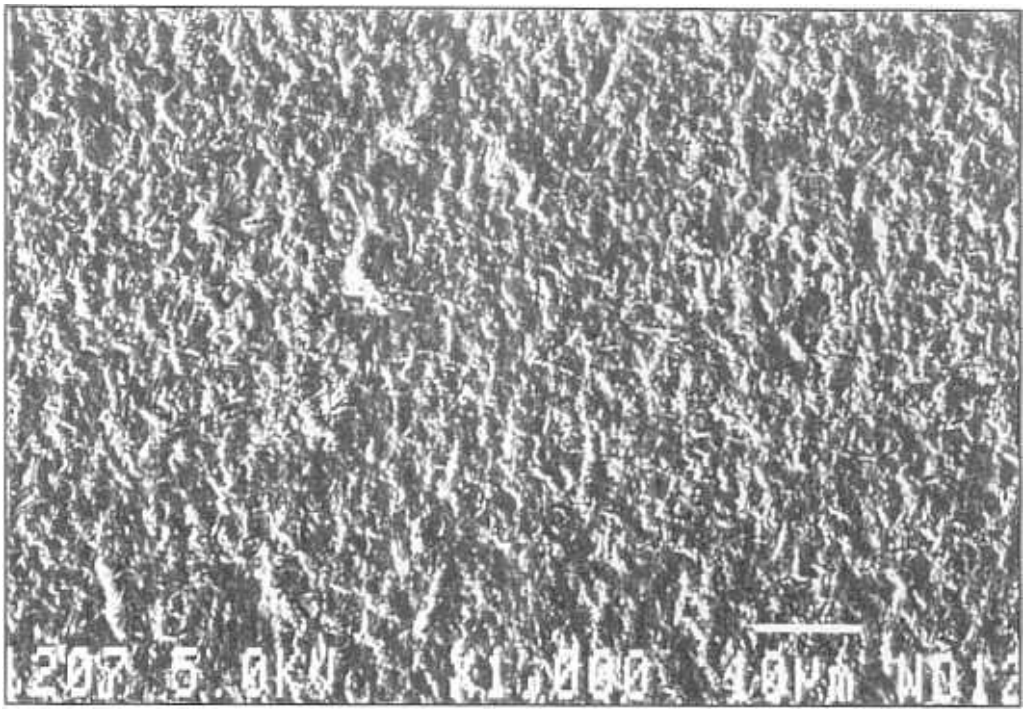

a)

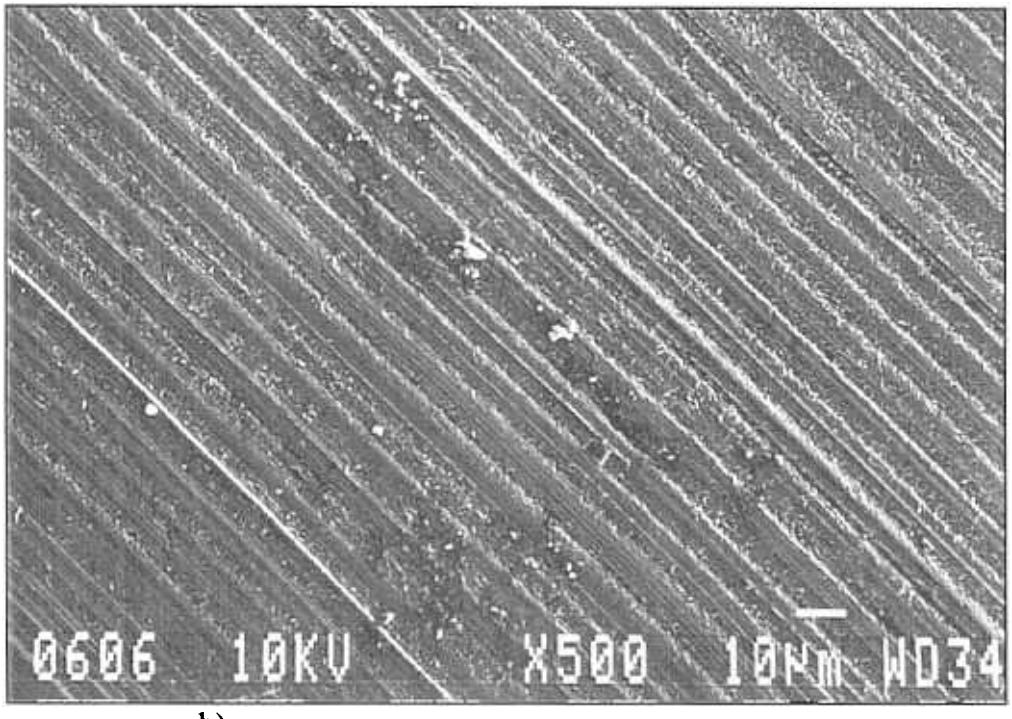

b)

Figure 19 Worn surfaces of tool steel samples tested with SiC abrasive a) in rolling wear regime, b) in grooving wear regime, ref [19].

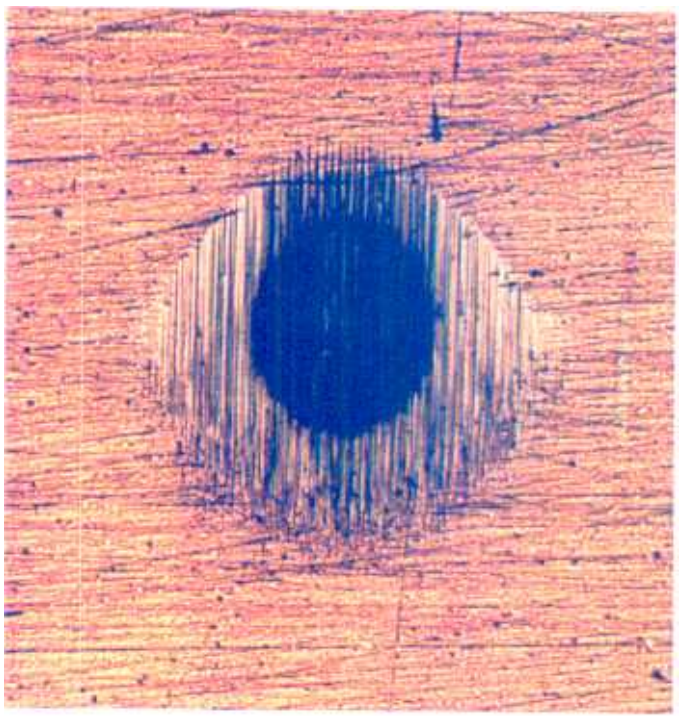

Figure 20 Overall appearance of TiN crater tested in grooving wear regime.

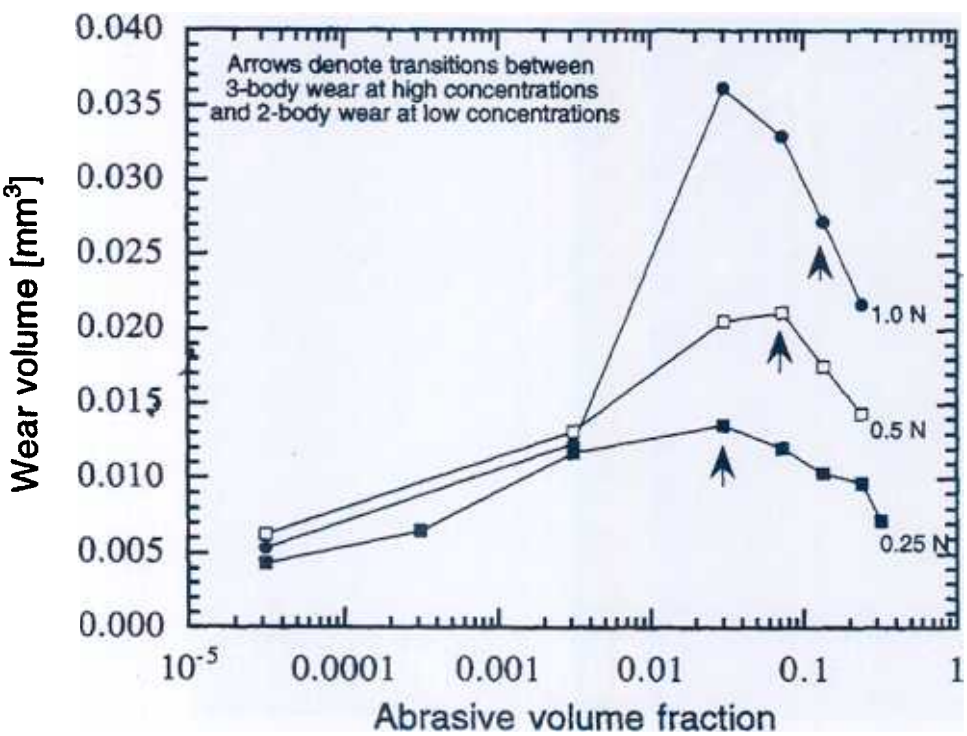

Figure 21 Variation in magnitude of wear of tool steel sample with SiC abrasive slurry concentration, ref [19].

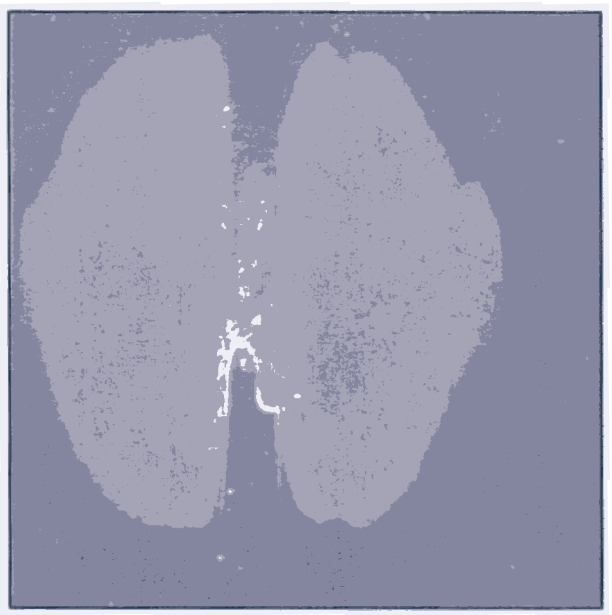

Figure 22 Ridge formed at centre of crater on TiN coated tool steel sample under high load dry sliding conditions.

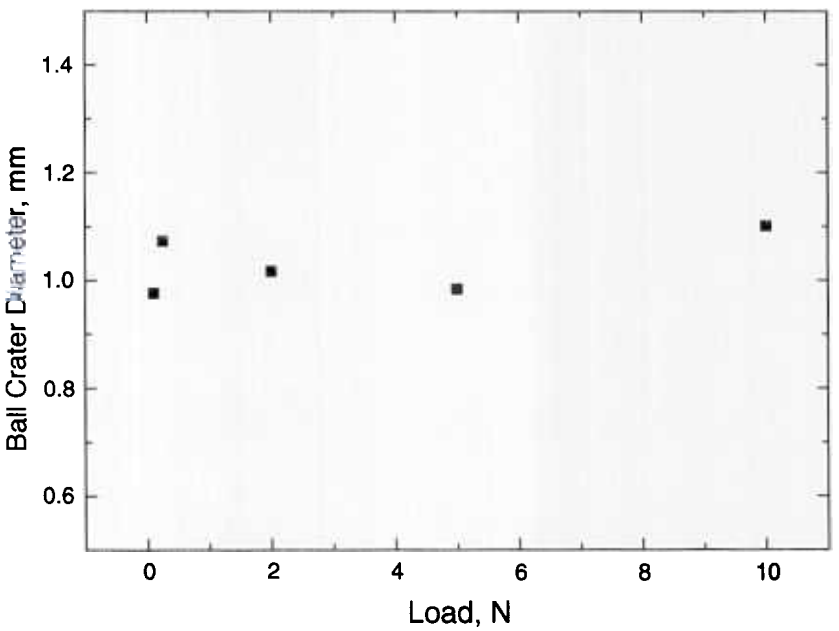

Figure 23, Lack of variation of wear with changing load for WC/Co sample tested with SiC abrasive. Lack of wear is correlated with increasing size of ridge.

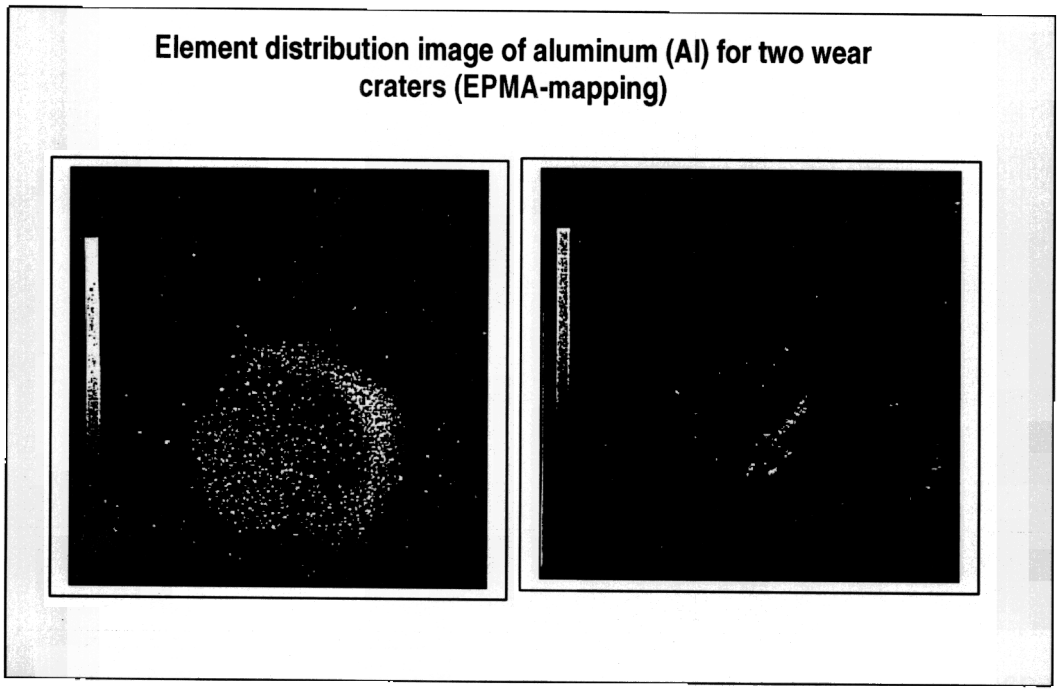

Figure 24 Embedding of alumina abrasive in the coating by high loading on left, no embedding on right with appropriate loading [8].

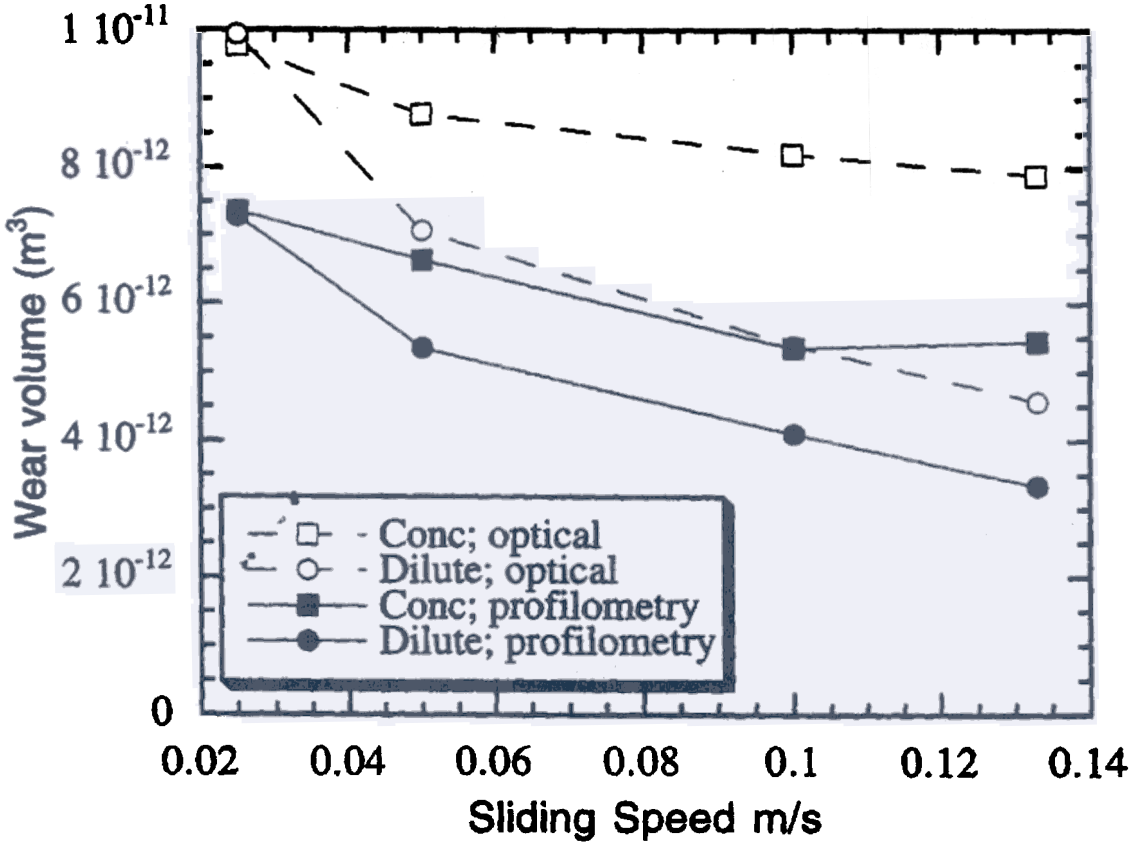

Figure 25 Variation in wear volume for tool steel sample with sliding speed, ref [13].

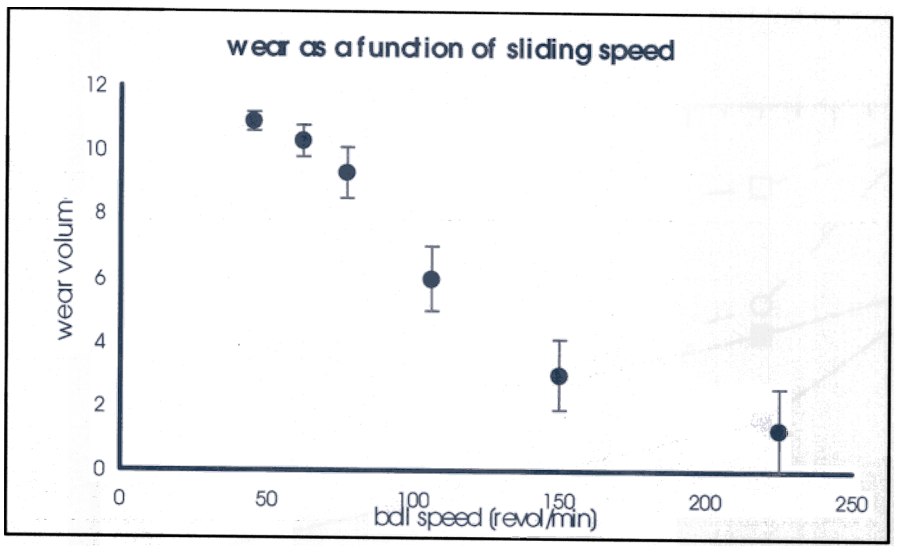

Figure 26 Effect of speed on apparent wear for free ball-single shaft machine with DLC coating and 1 μm diamond suspension.

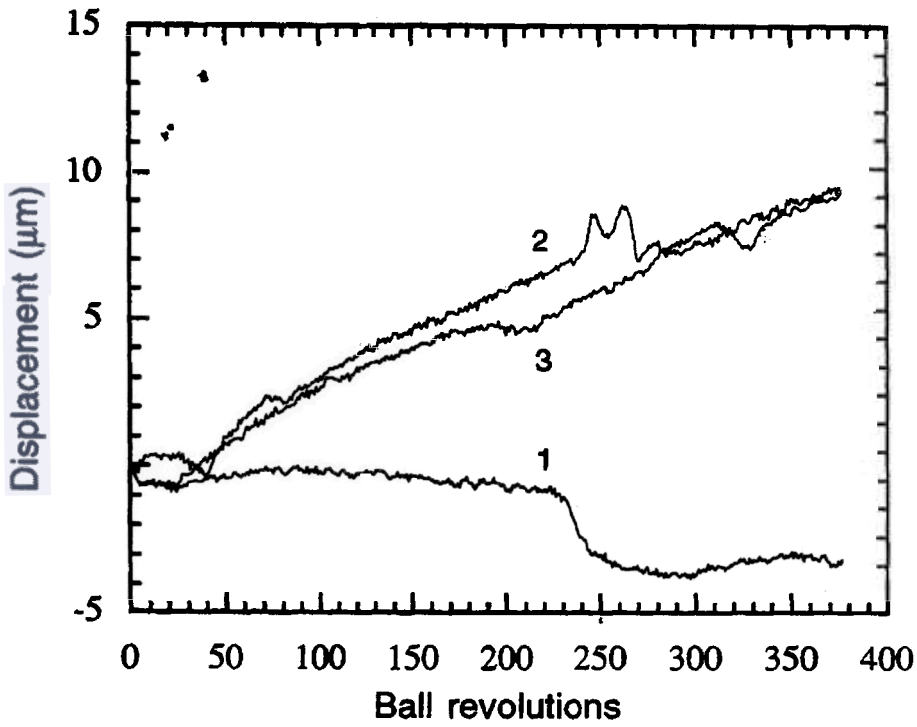

a)

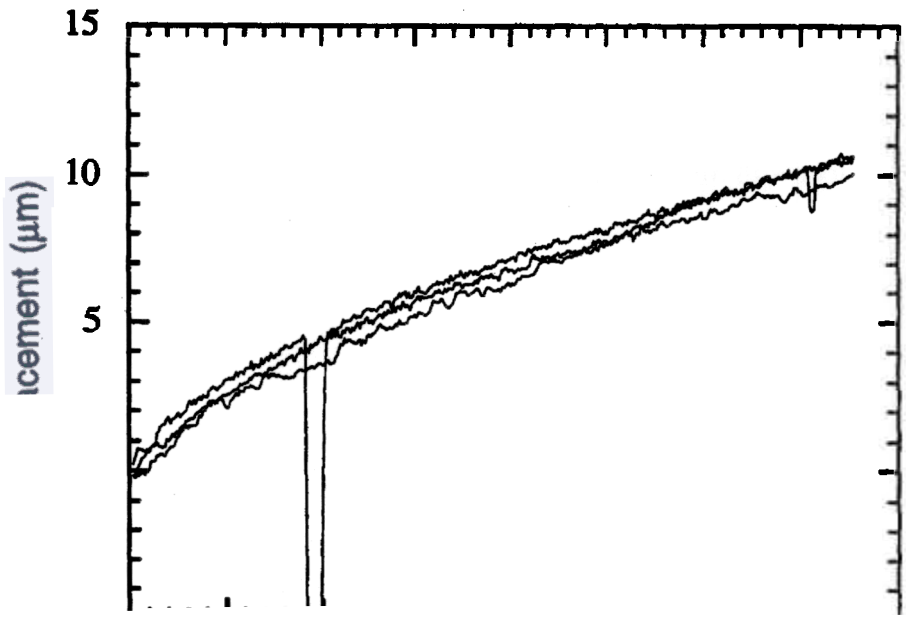

b)

Figure 27 Wear displacement traces for three repeat tests on silver steel with SiC abrasive, a) new test balls, b) used test balls, ref [20].

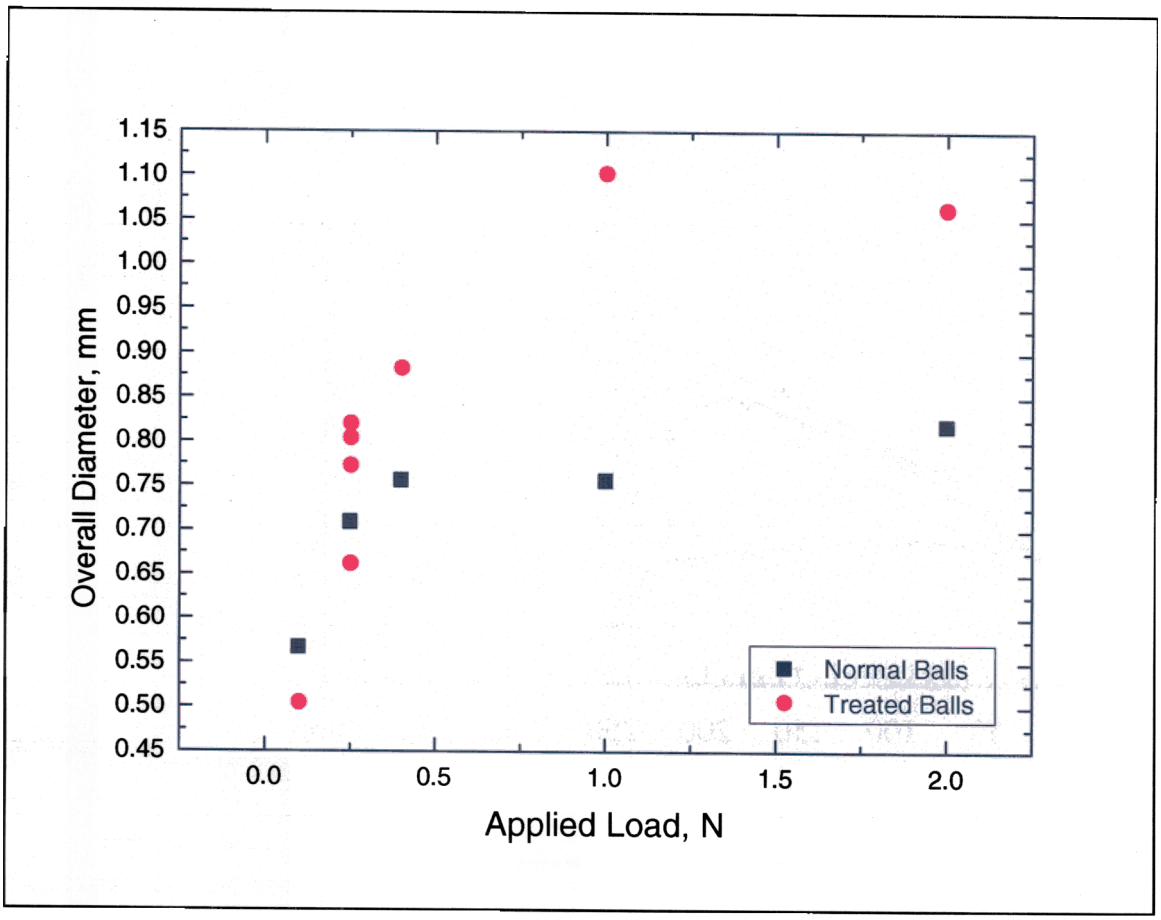

Figure 28 Increase in wear for treated balls by comparison with new balls. Tests on TiN coated tool steel with SiC abrasive.

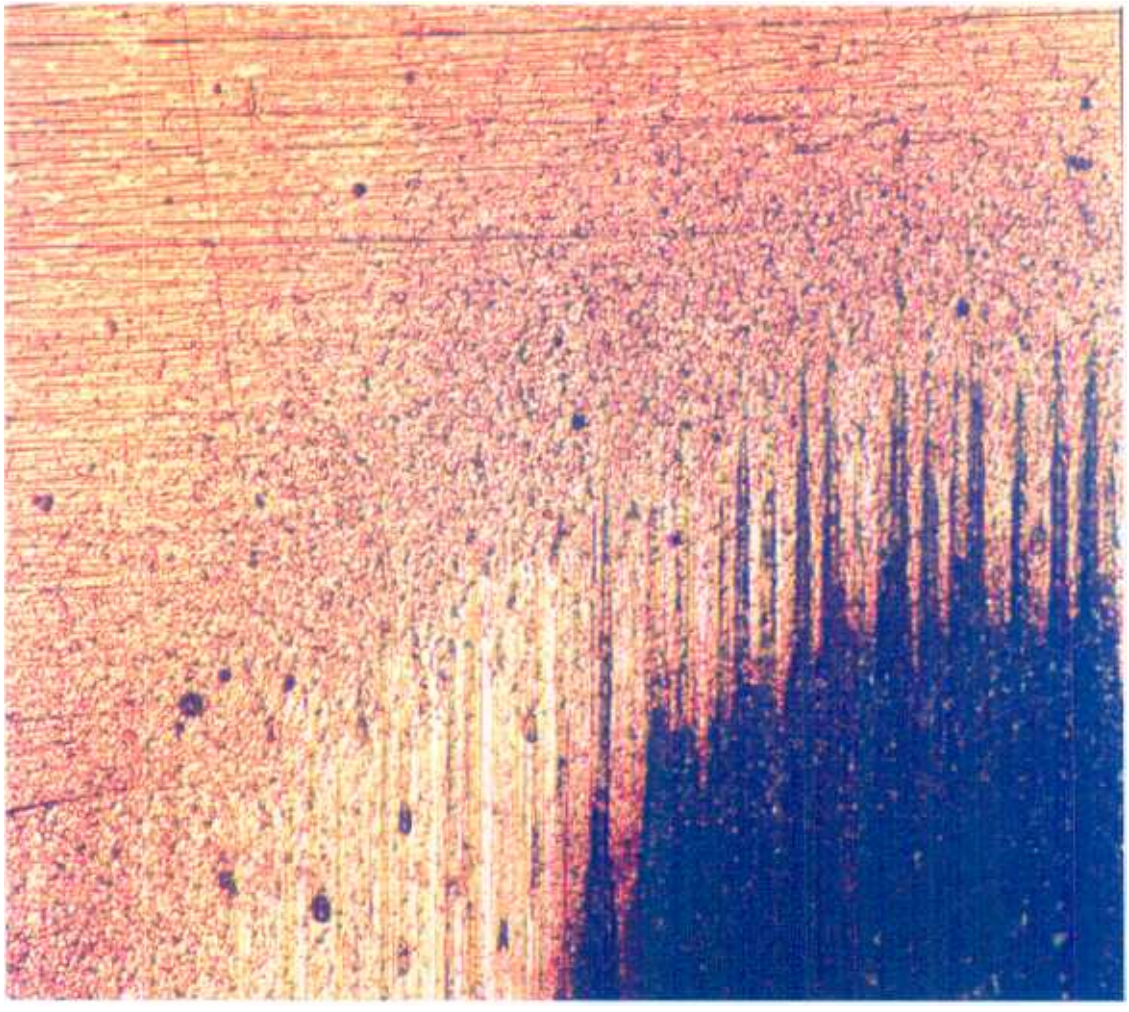

Figure 29 Poorly defined edge of crater.

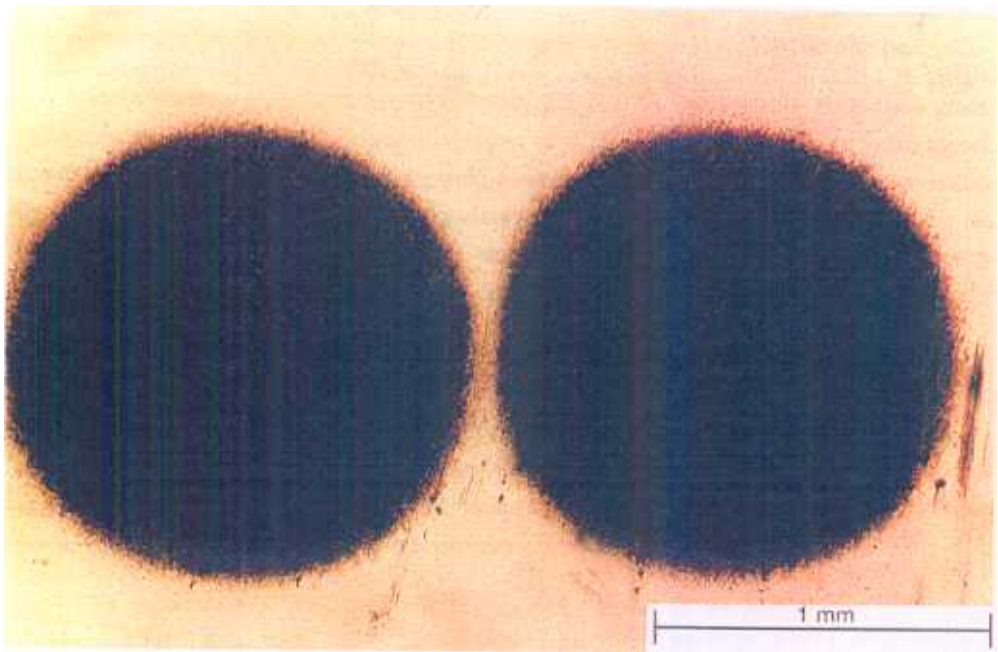

a)

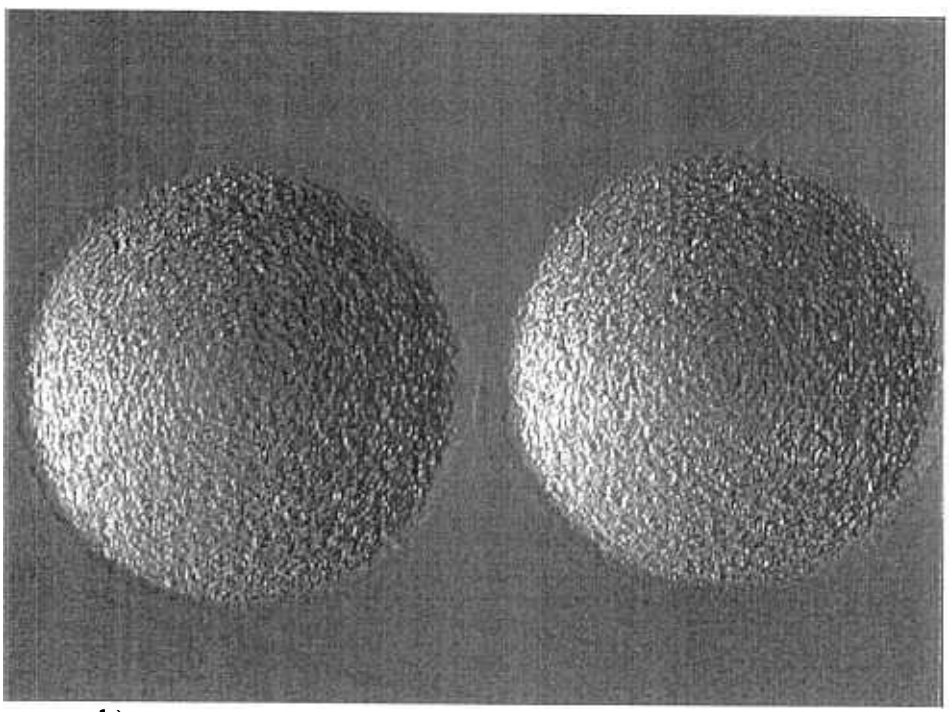

b)

Figure 30 Twin (same test conditions) craters on tool steel sample, a) optical micrograph, b) height map from profilometric measurement, ref [13].

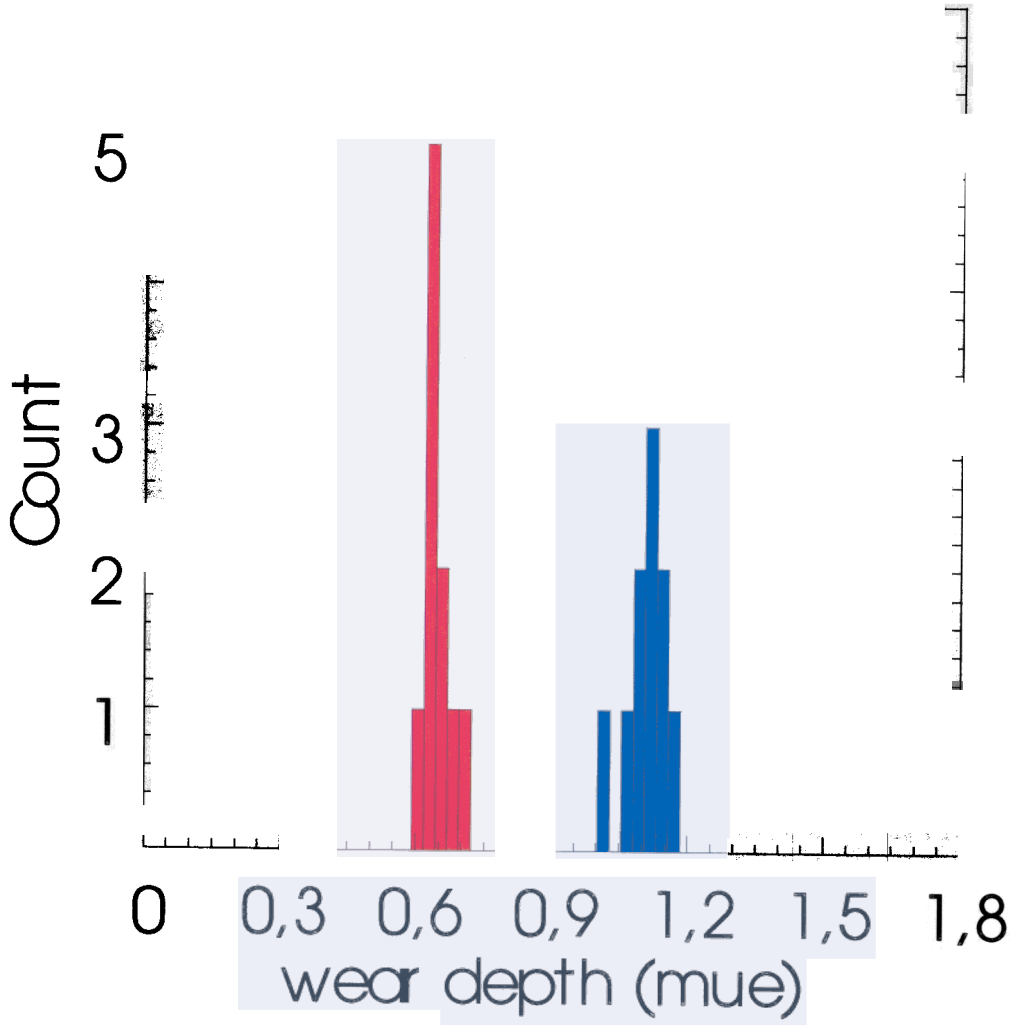

Figure 31 Repeatability of non-perforating ball crater tests on free-ball-single shaft system [8]

ANNEX: BIBLIOGRAPHY

1. Allsopp D N; Trezona R I; Hutchings I M, The effects of ball surface condition in the micro-scale abrasive wear test, TRIBOLOGY LETTERS 1998, Vol 5, Iss 4, pp 259-264
2. Andersen P; Bottiger J; Dyrbye K; Hutchings I M; rutherford K L; Wroblewski A, Mechanical properties of amorphous Ta100-xCrx thin films, MATERIALS SCIENCE AND ENIGNEERING A-STRUCTURAL MATERIALS PROPERTIES MICROSTRUCTURE AND PROCESSING 1997, Vol 226, pp 871-873
3. Axen N; Jacobson; Hogmark S, Principles for the tribological evaluation of intrinsic coating properties, WEAR 1997, Vol 203, pp 637-641
4. Bellido-Gonz V; Hampshire J; Jones A;, Advances in the analysis and characterization of DLC coatings, Surf. Coat. 98 1-Mar (1998) 1272-1279
5. Bethke R; Eder M;, PrazisionverschleiBmessungen an dunnen Schichten als Mittel zur Qualitatssicherung und Schichtentwicklung, Mat.-wiss. U. Werkstofftechnik 31, 1056-1059 (2000)
6. Bewilogua K; Cooper C V; Specht C; Schroder J; Wittorf R; Grischke M;, Effect of target material on deposition and properties of metal-containing coatings, Surf. Coat. Technol. 127 (2000) 224-232
7. Bewilogua K; Grischke M; Schroder J; Specht C; Michler T; van der Kolk G J; Trinh T; Hurkmans T; Fleicher W;, High Performance Me-DLC Coatings for Precision Components, Society of Vacuum Coaters 505/856-7188
8. Bromark M; Gahlin R; Hedenqvist P; Hogmark s; Hakansson G; Hansson G, Influence of recoating on the mechanical and tribological performance of TiN-coated HSS, SURFACE & COATINGS TECHNOLOGY 1995, Vol 77, Iss 1-3, pp 481-486
9. Bromark M; Larsson M; Hedenqvist P; Hogmark S, Wear of PVD Ti/TiN multilayer coatings, SURFACE & COATINGS TECHNOLOGY 1997, Vol 90, Iss 3, pp 217-223
10. Chen H; Hutchings I, Abrasive wear resistance of plasma-sprayed tungsten carbide cobalt coatings, Surf. Coat. 107 2-Mar (1998) 106-114
11. Choudhury M; Hutchings I M, The effects of irradiation and ageing on the abrasive wear resistance of ultra high molecular weight polyethylene, WEAR 1997, Vol 203, pp 335-340
12. Diserens M; Patscheider J; Levy F, Improving the properties of titanium nitride by incorporation of silicon, SURFACE & COATINGS TECHNOLOGY 1998, Vol 109, Iss 1-3, pp 241-246
13. Eckardt T; Bewilogua K; van der Kolk G; Hurkmans T; Trinh T; Fleicher W;, Improving tribological properties of sputtered boron carbide coatings by process modifications, Surf. A. Coat. Technology 126 (2000) 69-75
14. Fox V; Hampshire J; Teer D;, MoS2/metal composite coatings deposited by closed-field unbalanced magnetron sputtering: tribological properties and industrial, Surf. Coat. 112 1-Mar (1999) 118-122
15. Gahlin R; Bromark M; Hedenqvist P; Hogmark S; Hakansson G, Properties of TiN and CrN coatings deposited at low temperature using reactive arc-evaporation, SURFACE & COATINGS TECHNOLOGY 1995, Vol 76, Iss 1-3, pp 174-180
16. Gahlin R; Larsson M; Hedenqvist P; Jacobson S; Hogmark S, The crater grinder method as a means for coating wear evaluation - An update, SURFACE & COATINGS TECHNOLOGY 1997, Vol 90, Iss 1-2, pp 107-114

17. Gee M G; Wicks M J, Ball crater testing for the measurement of the unlubricated sliding wear of wear-resistant coatings, SURFACE & COATINGS TECHNOLOGY 2000, Vol 133, pp 376-382
18. Grigorescu I; Ramirez J; Salcedo F;, Tribological behavior of vanadium oxicarbide coatings, Surf. Coat. 94-5 1-Mar 1997 437-440
19. Hedenqvist P; Bromkar M; Olsson M; Hogmark S; Bergmann E, Mechanical and Tribological Characterization of Low-temperature Deposited PVD Tin Coatings, SURFACE & COATINGS TECHNOLOGY 1994, Vol 63, Iss 2, pp 115-122
20. Hieke A; Bewilogua K; Taube K; Bialuch I; Waigel K;, Efficient Deposition for diamond-like Carbon Coatings, Society of Vacuum Coaters 505/856-7188 Page 301-304
21. Hoffmann H; Schuessler K; Bewilogua K; Hubsch H; Lemke J;, Plasma-booster hydrogenated W-C coatings, Surf. A. Coat. Technology 73 (1995) 137-141
22. Hogmark S; Hedenqvist P, Tribological Characterization of Thin, Hard Coatings, WEAR 1994, Vol 179, Iss 1-2, pp 147-154
23. Hogmark S; Hedenqvist P; Jacobson S, Tribological properties of thin hard coatings: Demands and evaluation, SURFACE & COATINGS TECHNOLOGY 1997, Vol 90, Iss 3, pp 247-257
24. Hogmark S; Jacobson S; Larsson M, Design and evaluation of tribological coatings, WEAR 2000, Vol 246, Iss 1-2, pp 20-33
25. Hollman P; Hedenqvist P; Hogmark S; Stenberg G; Boman M, Tribological evaluation of thermally activated CVD diamond-like carbon (DLC) coatings, SURFACE & COATINGS TECHNOLOGY 1997, Vol 96, Iss 2-3, pp 230-235
26. Imbeni V; Hutchings I M; Breslin M C, Abrasive wear behaviour of an Al203-Al co-continuous composite, WEAR 1999, Vol 235, pp 462-467
27. Jones A; Camino D; Teer D;, Novel high wear resistant diamond-like carbon coatings deposited by magnetron sputtering of carbon targets, Proc. Inst. Mech. Eng. Part J.-J. Eng. Tribol.212 J4 1998 301-306
28. Larsson M; Bromark M; Hedenqvist P; Hogmark S, Mechanical and tribological properties of Multilayered PVD TiN/NbN coatings, SURFACE & COATINGS TECHNOLOGY 1997, Vol 91, Iss 1-2, pp 43-49
29. Larsson P; Axen N; Ekstrom T; Gordeev S; Hogmark S, Wear of a new type of diamond composite, INTERNATIONAL JOURNAL OF REFRACTORY METALS & HARD MATERIALS 1999, Vol 17, Iss 6, pp 453-460
30. Ljungscrantz H; Engstrom C; Hultman L;, Nanoindentation hardness, abrasive wear, and microstructure of TiN/NbN polycrystalline nanostructured multilayer films grown by, J. Vac. Sci. 16 5 (1998) 3104-3113
31. Lou H Q; Axen N; Somekh R E; Hutchings I M, Mechanical properties of amorphous carbon nitride films, DIAMOND AND RELATED MATERIALS 1996, Vol 5, Iss 11, pp 1303-1307
32. Maier M; Viefhaus H; Grabke H;, SCANNING AUGER ANALYSIS FOR THE CLARIFICATION OF OXIDATION AND INTERDIFFUSION PROCESSES DURING LASER-ABLATION OF YBA2CU3O7-X ON, Fresenius 353 5-Aug (1995) 675-677
33. Mehner A; Klumper-W H; Hoffmann F;, Crystallization and residual stress formation of sol-gel- derived zirconia films, Thin Solid 308 (1997) 363-368
34. Meneve J; Havermans D; Vercammen K; Haefke H; Gerbig Y: Pfluger E, Mechanical properties and tribological behaviour of state-of-the-art diamond-like carbon

coatings, ADVANCED ENGINEERING MATERIALS 2001, Vol 3, Iss 3, pp 163-166

35. Michler T; Grischke M; Traus I; Bewilogua K; Dimigen H;, Mechanical properties of DLC films prepared by bipolar pulsed DC PACVD, Diamond and Related Materials 7 (1998) 1333-1337
36. Munz W D; Donohue L A; Hovsepian P E, Properties of various large-scale fabricated TiAlN- and CrN-based superlattice coatings grown by combined cathodic arc-unbalanc, SURFACE & COATINGS TECHNOLOGY 2000, Vol 125, Iss 1-3, pp 269-277
37. Nig Y; Xie H; Zhan J, Depth-profiling of Ti/Mo films of micrometer thickness by AES, J. Trace M 15 4 (1997) 585-588
38. Nordin M; Larsson M; Hogmark S, Mechanical and tribological properties of multilayered PVD TiN/CrN, WEAR 1999, Vol 232, Iss 2, pp 221-225
39. Nordin M; Larsson M; Hogmark S, Mechanical and tribological properties of multilayered PVD TiN/CrN, TiN/MoN, TiN/NbN and TiN/TaN coatings on cemented carbide, SURFACE & COATINGS TECHNOLOGY 1998, Vol 106, Iss 2-3, pp 234-241
40. Nordin M; Larsson M; Hogmark S;, Wear resistance of multilayered PVD TiN/TaN on HSS, Surf. Coat. 121 (1999) 528-534
41. Nothnagel G, Wear-resistance Determination of Coatings from Cross-section Measurements of Ball-ground Craters, SURFACE & COATINGS TECHNOLOGY 1993, vol 57, Iss 2-3, pp 151-154
42. Okumiya M; Griepentro M, Mechanical properties and tribological behavior of TiN-CrAlN and CrN-CrAlN multilayer coatings, Surf. Coat. 112 1-Mar 1999 123-128
43. Pfluger E; Schroer A; Voumard P;, Influence of incorporation of Cr and Y on the wear performance of TiAlN coatings at elevated temperatures, Surf. Coat. 115 1 (1999) 17-23
44. Ramirez J; Grigorescu I; Weil C;, Vanadium oxicarbide thin films prepared by conventional chemical vapor deposition from vanadyl acetylacetonate, Surf. Coat. 94-5 1-Mar (1997) 441-445
45. Richter J; Hutchings I M; Clyne T W; Allsopp D N; Peng X, Tribological characterization of diamond-like carbon films on nonledeburitic high-speed steels, MATERIALS CHARACTERIZATION 2000, Vol 45, Iss 3, pp 233-239
46. Robson J; James A; Matthew A;, THE DEPOSITION OF YTTRIA PARTIALLY-STABILIZED ZIRCONIA (PYSZ) ONTO ALUMINUM-ALLOY SUBSTRATES USING PVD TECHNIQUES, Surf. Coat. 60 1-Mar (1993) 536-540
47. Rother B; Jehn H; Gabriel H, Multilayer hard coatings by coordinated substrate rotation modes in industrial PVD deposition systems, Surf. Coat. 87-8 1-Mar (1996) 207-211
48. Runge, M, Optimierung eines Testgerates zur abrasiven VerschleiBmessung, FhG-1st,
49. Rutherford K L; Bull S J; Doyle E D; Hutchings I M, Laboratory characterisation of the wear behaviour of PVD-coated tool steels and correlation with cutting tool performance, SURFACE & COATINGS TECHNOLOGY 1996, Vol 80, Iss 1-2, pp 176-180
50. Rutherford K L; Hatto P W; Davies C; Hutchings I M, Abrasive wear resistance of TiN/NbN multi-layers: Measurement and neural network modelling, SURFACE & COATINGS TECHNOLOGY 1996, vol 86-7, Iss 1-3, pp 472-479

51. Rutherford K L; Hutchings I M, A micro-abrasive wear test, with particular application to coated systems, SURFACE & COATINGS TECHNOLOGY 1996, Vol 79, Iss 1-3, pp 231-239
52. Rutherford K L; Hutchings I M, Theory and application of a micro-scale abrasive wear test, JOURNAL OF TESTING AND EVALUATION 1997, Vol 25, Iss 2, pp 250-260
53. Rutherford K L; Hutchings I M, Development of the erosion durability technique for thin coatings, SURFACE & COATINGS TECHNOLOGY 1996, Vol 86-7, Iss 1-3, pp 542-548
54. Rutherford K L; Hutchings I M;, Micro-scale abrasive wear testing of PVD coatings on curved substrates, Tribology Letters 2 (1996) 1-11
55. Rutherford K L; Trezona R I; Ramamurthy A C; Hutchings I M, The abrasive and erosive wear of polymeric pain films, WEAR 1997, Vol 203, pp 325-334
56. Shipway P H, The role of test conditions on the microabrasive wear behaviour of soda-lime glass, WEAR 1999, Vol 235, pp 191-199
57. Shipway P H; Hodge C J B, Microabrasion of glass - the critical role of ridge formation, WEAR 2000, Vol 237, Iss 1, pp 90-97
58. Siebert, C, Entwicklung eines VerschleiBtesters fur dunne Schichten am Beispiel amorpher Kohlenstoffschichten, FhG-IST,
59. Smolik J; Zdunek K, Effect of interlayer composition on the tribological properties of TiC/Ti(C-x, N1-x)/TiN anti-abrasive multi-layer coatings, VACUUM 1999, Vol 55, Iss 2, pp 147-151
60. Staia M H; Enriquez C; Puchi E S, Influence of the heat treatment on the abrasive wear resistance of electroless Ni-P, SURFACE & COATINGS TECHNOLOGY 1997, Vol 94-5, Iss 1-3, pp 543-548
61. Staia M; Lewis B; Cawley J;, Chemical vapour deposition of TiN on stainless steel, Surf. Coat. 76 1-Mar (1995) 231-236
62. Taube T;, Carbon-based coatings for dry sheet-metal working, Surf. A. Coat. Tech. 98 (1998) 976-984
63. Trezona R I; Allsopp D N; Hutchings I M, Transitions between two-body and three-body abrasive wear; influence of test conditions in the microscale abrasive wear test, WEAR 1999, Vol 229, pp 205-214
64. Trezona R I; Hutchings I M, Three-body abrasive wear testing of soft materials, WEAR 1999, Vol 235, pp 209-221
65. Voumard P; Jeanpetit E;, Le calowear comme test d'usure abrasive pour les revetements durs,
66. Wanstrand O; Larsson M; Hedenqvist P;, Mechanical and tribological evaluation of PVD WC/C coatings, Surf. Coat. 111 2-Mar (1999) 247-254
67. Yamamoto Kenji; Keunecke M; Bewilogua K;, Adhesion Improvement of cBN film by B_C_N Gradient Layer System, New Diamond and Frontier Carbon Technology, Vol 10, No 4 2000